Physical interpretations

Time reversal

Rays and stationary phase

Example: an even uncorrelated distribution of source (acoustic case) (Roux et al., 2004)

$$C_{12}(\tau) = \int_{-\infty}^{\infty} P(\mathbf{r}_1, t)\, P(\mathbf{r}_2, t+\tau)\,\mathrm{d}\,t. \quad \text{where,}$$

$$P(\mathbf{r}_i, t) = \int_0^{\infty} d\mathbf{r}_s \int_{-\infty}^{t} dt_s\;\; S(\mathbf{r}_s; t_s) g(\mathbf{r}_s, \mathbf{r}_i; \mathrm{t - ts});\; \mathrm{i} = 1,2.$$

1. Finite recording time T_r
2. Uncorrelated noise sources: $< S(\mathbf{r}_s; t_s) S(\tilde{\mathbf{r}}_s; t_s) >= Q^2 \upsilon \delta(\mathbf{r}_s - \tilde{\mathbf{r}}_s) \delta(t_s, \tilde{t}_s)$
3. Change variable: $\hat{\mathrm{t}} = \mathrm{t} - \mathrm{t_s}$

$$C_{12}(\tau) = Q^2 \upsilon T_r \underbrace{\int_0^{\infty} d\mathbf{r}_s}_{\text{Spatial sum}} \underbrace{\int_0^{\infty} \mathrm{d}\,\hat{\mathrm{t}}\, g(\mathbf{r}_s, \mathbf{r}_1; \hat{\mathrm{t}})\, g(\mathbf{r}_s, \mathbf{r}_2; \hat{\mathrm{t}} + \tau)}_{\text{Cross-correlation for each noise source}}.$$

Noise cross-correlation: Free space

Noise sources yielding constant time-delay τ, lay on same Hyperbola

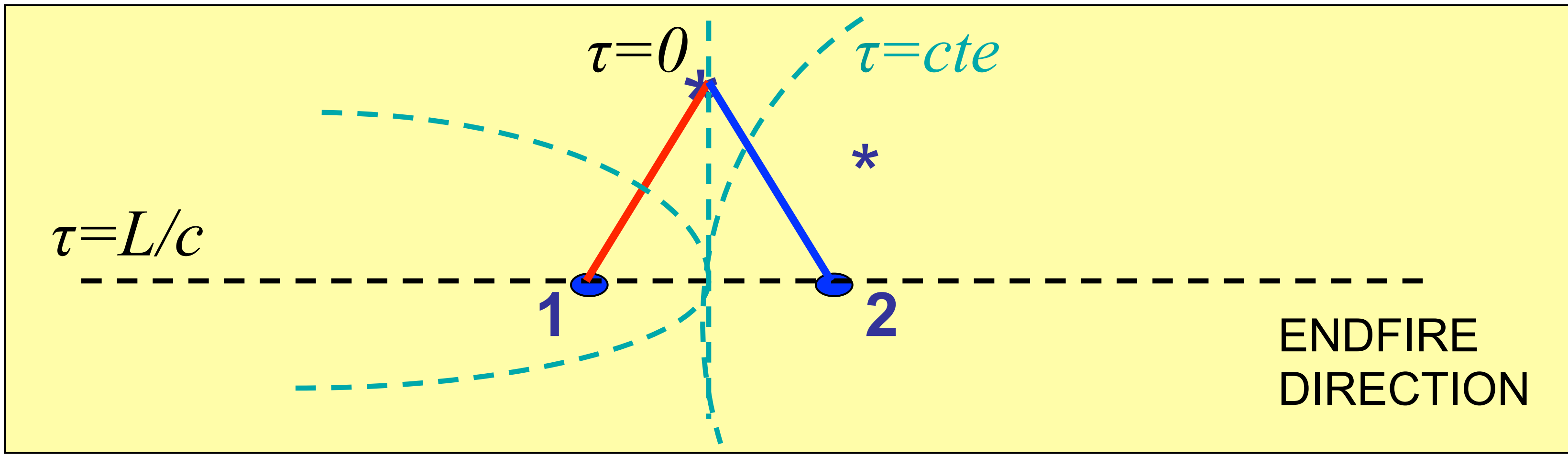

$$\tau = \frac{|\mathbf{r}_1 - \mathbf{r}_s| - |\mathbf{r}_2 - \mathbf{r}_s|}{c} \le \frac{L}{c}$$

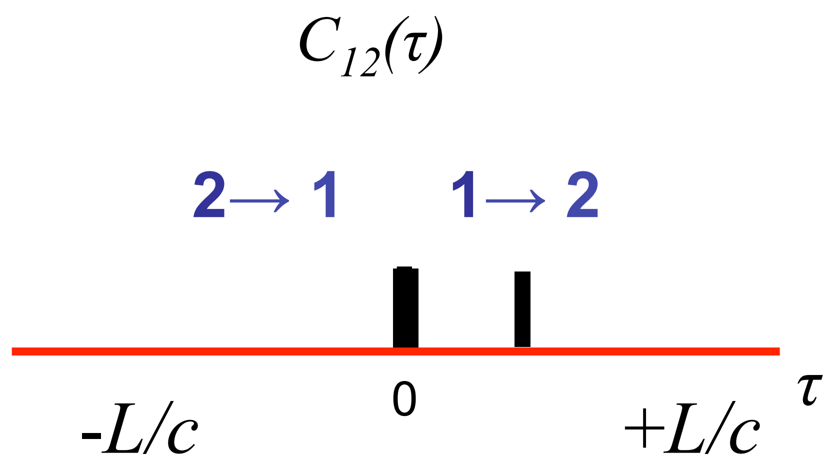

Isotropic distribution of uncorrelated random noise sources

C, dC/dt, band-limited signal

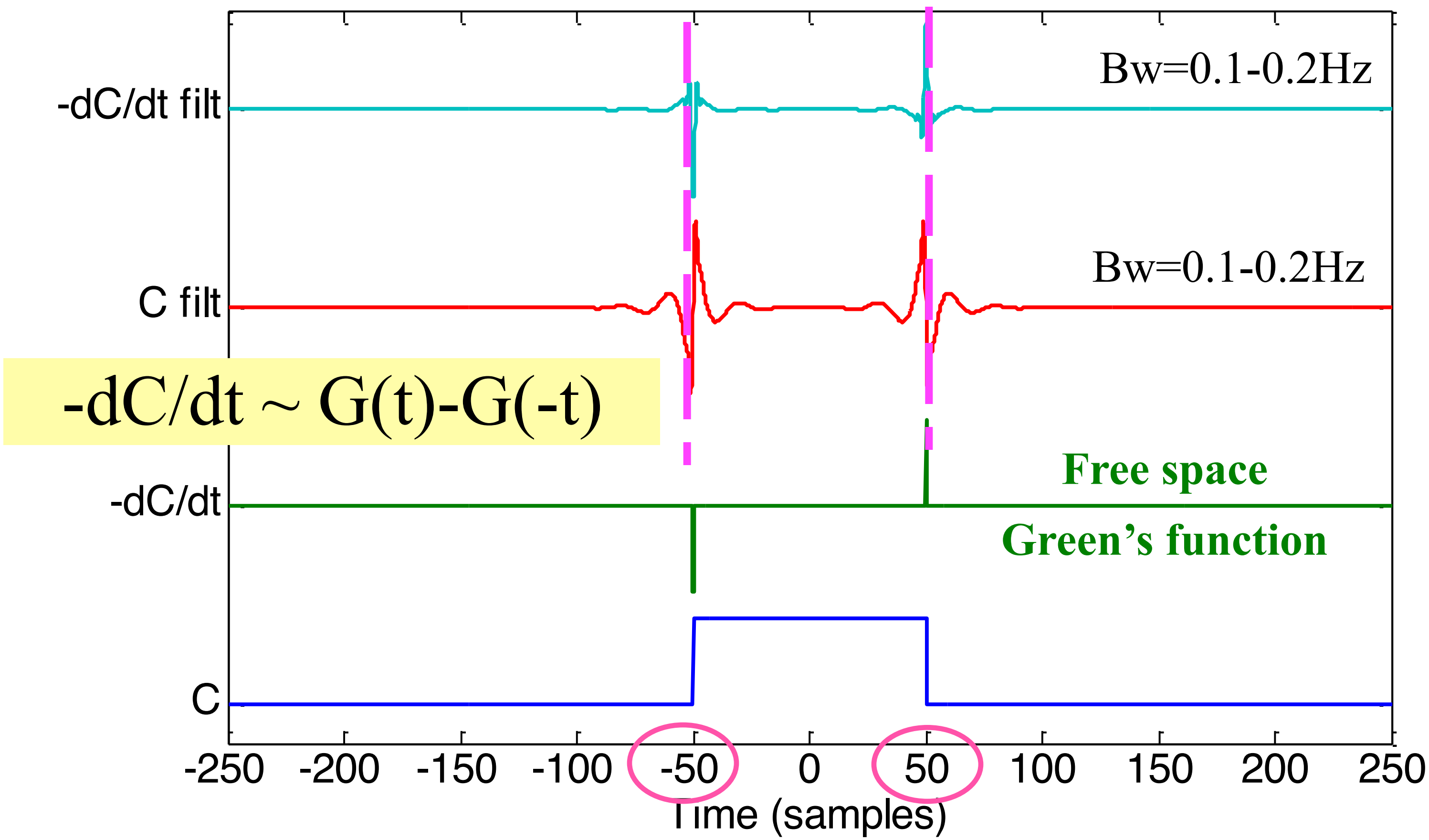

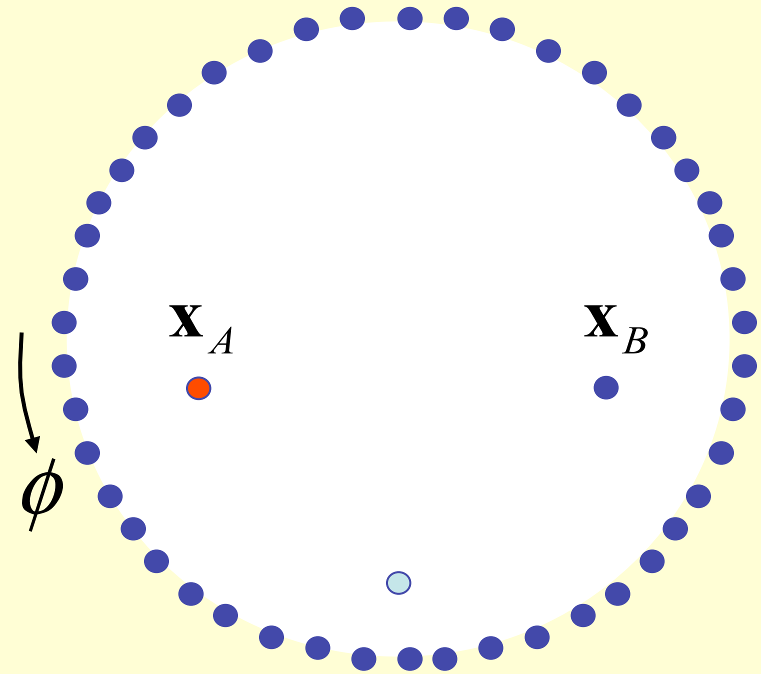

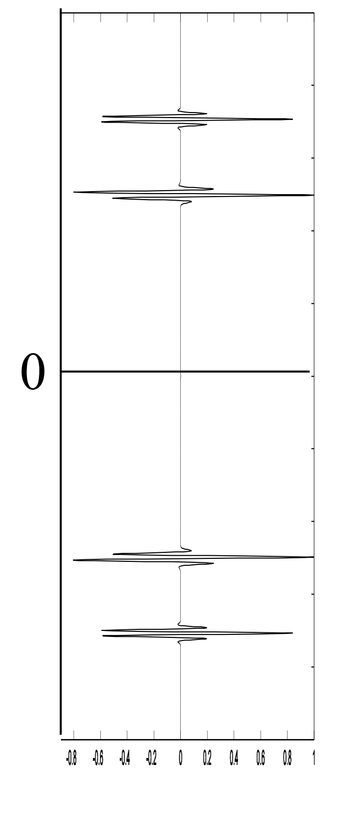

$$G(\mathbf{x}_B,\mathbf{x}_A,t)+G(\mathbf{x}_B,\mathbf{x}_A,-t)\approx \frac{2}{\rho c}\int_S G(\mathbf{x}_B,\mathbf{x},t)*G(\mathbf{x}_A,\mathbf{x},-t)d^2\mathbf{x}$$

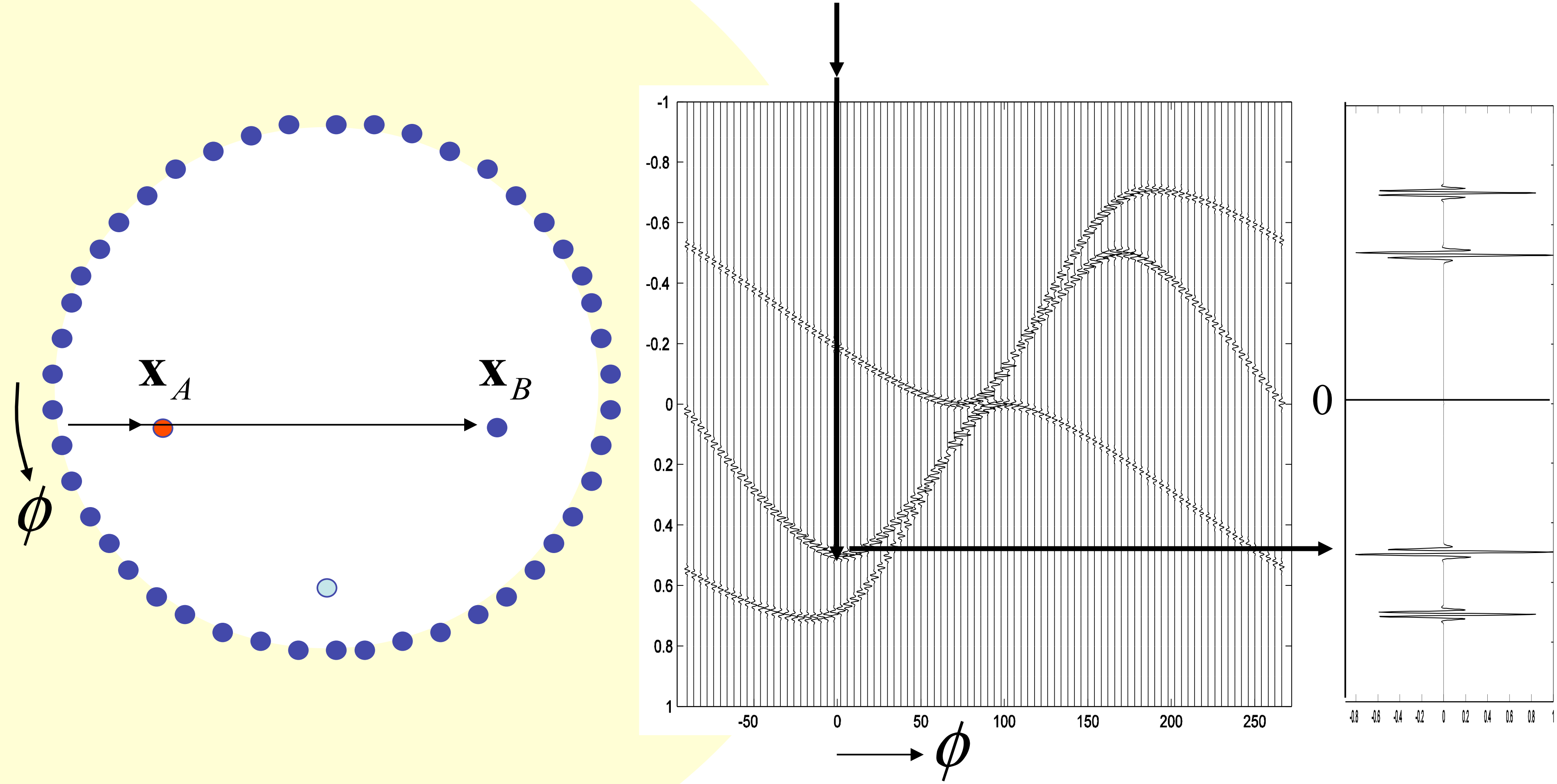

$$G(\mathbf{x}_B,\mathbf{x}_A,t)+G(\mathbf{x}_B,\mathbf{x}_A,-t) \approx$$

$$\frac{2}{\rho c}\int_S G(\mathbf{x}_B,\mathbf{x},t)*G(\mathbf{x}_A,\mathbf{x},-t)d^2\mathbf{x}$$

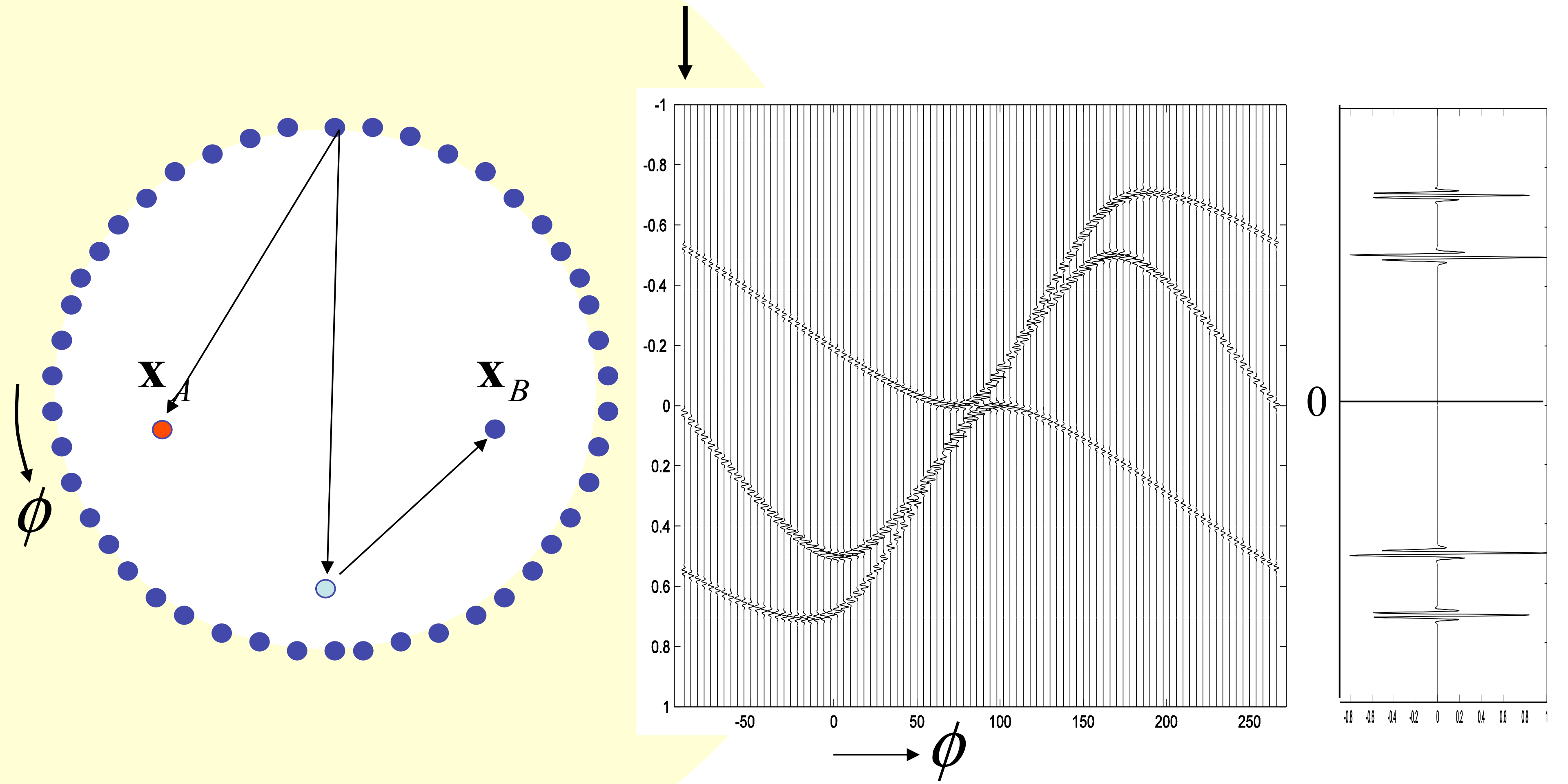

$$G(\mathbf{x}_B,\mathbf{x}_A,t)+G(\mathbf{x}_B,\mathbf{x}_A,-t) \approx \frac{2}{\rho c}\int_S G(\mathbf{x}_B,\mathbf{x},t)*G(\mathbf{x}_A,\mathbf{x},-t)d^2\mathbf{x}$$

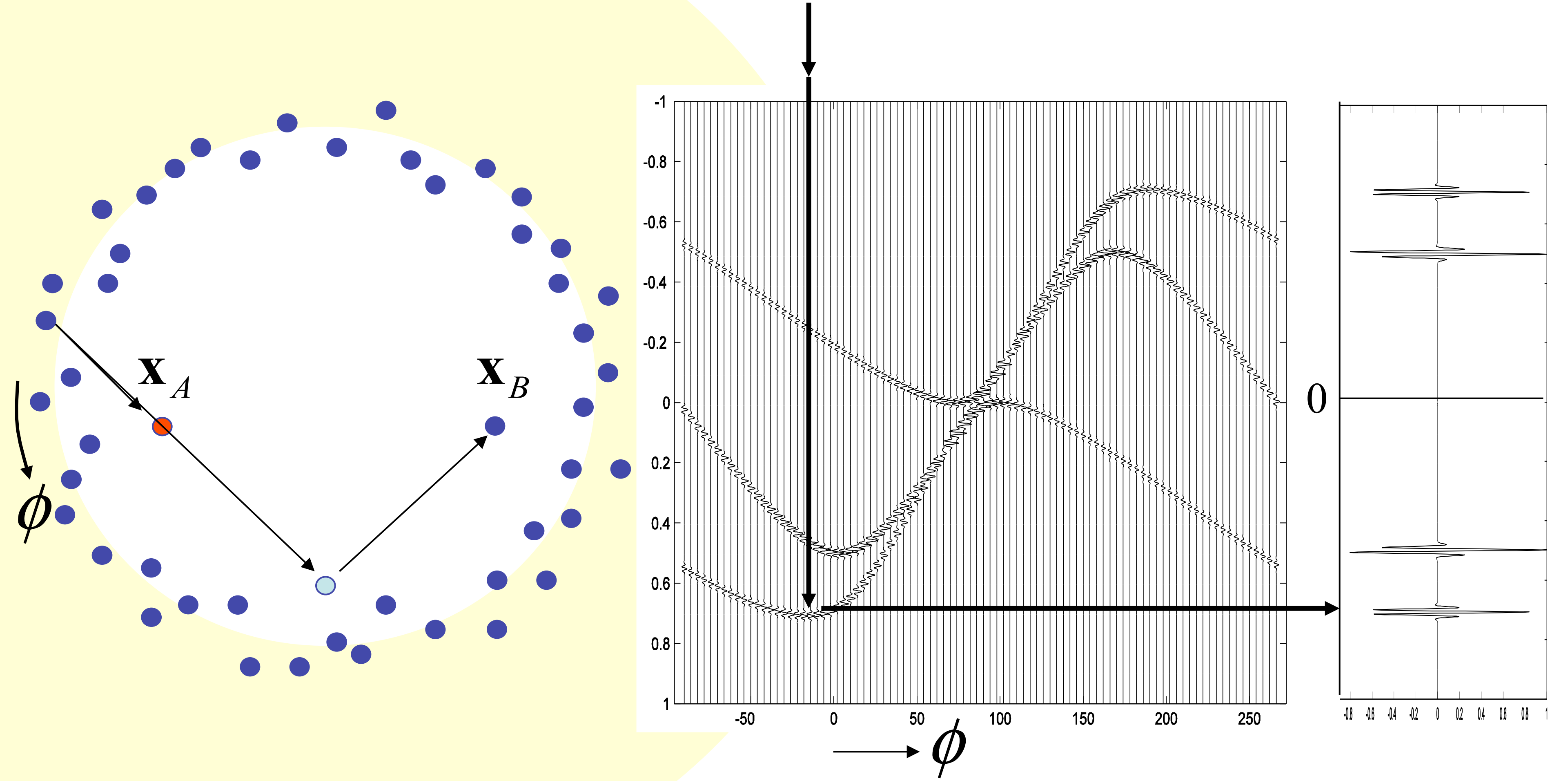

$$G(\mathbf{x}_B,\mathbf{x}_A,t)+G(\mathbf{x}_B,\mathbf{x}_A,-t) \approx \frac{2}{\rho c}\int_S G(\mathbf{x}_B,\mathbf{x},t)*G(\mathbf{x}_A,\mathbf{x},-t)d^2\mathbf{x}$$

Correlations, Green function and equipartition

Elasticity

P-SV case

Green function in 2D

$$G_{ij} = \frac{i}{4\rho\omega^2}\left\{-\delta_{ij}k^2 H_0^{(2)}(kr) + \frac{\partial^2}{\partial x_i \partial x_l}\left[H_0^{(2)}(qr) - H_0^{(2)}(kr)\right]\delta_{lj}\right\}$$

$$G_{ij}(P,Q) = \frac{-\mathrm{i}}{8\rho}\left\{A\delta_{ij} - B\left(2\gamma_i\gamma_j - \delta_{ij}\right)\right\} \qquad \gamma_j = \frac{x_j - \xi_j}{r}$$

$$A = \frac{H_0^{(2)}(qr)}{\alpha^2} + \frac{H_0^{(2)}(kr)}{\beta^2} \qquad B = \frac{H_2^{(2)}(qr)}{\alpha^2} - \frac{H_2^{(2)}(kr)}{\beta^2}$$

Hankel functions

$$q = \frac{\omega}{\alpha} \qquad k = \frac{\omega}{\beta} \qquad \alpha = \sqrt{\frac{\lambda + 2\mu}{\rho}} \qquad \beta = \sqrt{\frac{\mu}{\rho}} \qquad r = |P,Q|$$

THE 2D VECTOR CASE

$$\beta^2 \frac{\partial^2 u_i}{\partial x_j \partial x_j} + (\alpha^2 - \beta^2) \frac{\partial^2 u_j}{\partial x_i \partial x_j} = \frac{\partial^2 u_i}{\partial t^2}$$

Summation of P and S plane waves:

$$u_l(\mathbf{x},\omega,t) = P(\omega,\phi) n_l \exp(-\mathrm{i}\frac{\omega}{\alpha} x_j n_j) + S(\omega,\psi) m_l' \exp(-\mathrm{i}\frac{\omega}{\beta} x_j m_j)$$

Correlation:

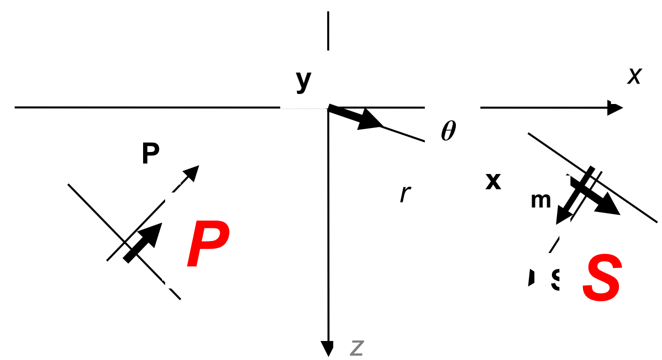

$$u_l(\mathbf{y}) u_s^*(\mathbf{x}) =$$

$$(P^2 n_l n_s + SP^* m_l' n_s) \exp(\mathbf{i} kr \cos[\phi - \theta]) +$$

$$(S^2 m_l' m_s' + PS^* n_l m_s') \exp(\mathbf{i} kr \cos[\psi - \theta])$$

$$u_1(\mathbf{y})u_1^*(\mathbf{x}) = (P^2\cos^2\phi - SP^*\sin\psi\cos\phi)\exp(\mathbf{i}qr\cos[\phi-\theta])$$
$$+(S^2\sin^2\psi + PS^*\cos\phi\sin\psi)\exp(\mathbf{i}kr\cos[\psi-\theta])$$

Azimuthal average:

$$\langle \bullet \rangle = \frac{1}{4\pi^2}\int_0^{2\pi} d\phi \int_0^{2\pi} \bullet \, d\psi$$

$$\langle u_1(\mathbf{y})u_1^*(\mathbf{x})\rangle = \frac{P^2\alpha^2}{2}\frac{J_0(qr)}{\alpha^2} + \frac{S^2\beta^2}{2}\frac{J_0(kr)}{\beta^2} -$$
$$-\frac{P^2\alpha^2}{2}\frac{J_2(qr)}{\alpha^2}\cos 2\theta + \frac{S^2\beta^2}{2}\frac{J_0(kr)}{\beta^2}\cos 2\theta$$

with $P^2\alpha^2 = \varepsilon S^2\beta^2$

$$\langle u_i(\mathbf{y})u_j^*(\mathbf{x})\rangle = \frac{S^2\beta^2}{2}\left\{A\delta_{ij} - B(2\gamma_i\gamma_j - \delta_{ij})\right\}$$

$$A = \varepsilon\frac{J_0(qr)}{\alpha^2} + \frac{J_0(kr)}{\beta^2} \text{ and } B = \varepsilon\frac{J_2(qr)}{\alpha^2} - \frac{J_2(kr)}{\beta^2}$$

$$P^2\alpha^2 = \varepsilon S^2\beta^2$$

Equipartition (*ε*=1):

$$E_S / E_P = \left(\frac{\alpha}{\beta}\right)^2$$

$$\left\langle u_i(\mathbf{y})u_j^*(\mathbf{x})\right\rangle = \frac{S^2\beta^2}{2}\left\{A\delta_{ij} - B(2\gamma_i\gamma_j - \delta_{ij})\right\}$$

$$A = \varepsilon\frac{J_0(qr)}{\alpha^2} + \frac{J_0(kr)}{\beta^2} \text{ and } B = \varepsilon\frac{J_2(qr)}{\alpha^2} - \frac{J_2(kr)}{\beta^2}$$

$$\downarrow$$

$$\boxed{\left\langle u_i(\mathbf{y},\omega)u_j^*(\mathbf{x},\omega)\right\rangle = -8E_S k^{-2}\,\mathrm{Im}\left[G_{ij}(\mathbf{x},\mathbf{y},\omega)\right]}$$

Formally, same result in 3D (Sánchez-Sesma and Campillo, 2006)

Correlations, Green function and equipartition

Locally heterogeneous body

SH waves in a medium with a cylindrical cavity

Analytical solution for the 2D SH Green function:

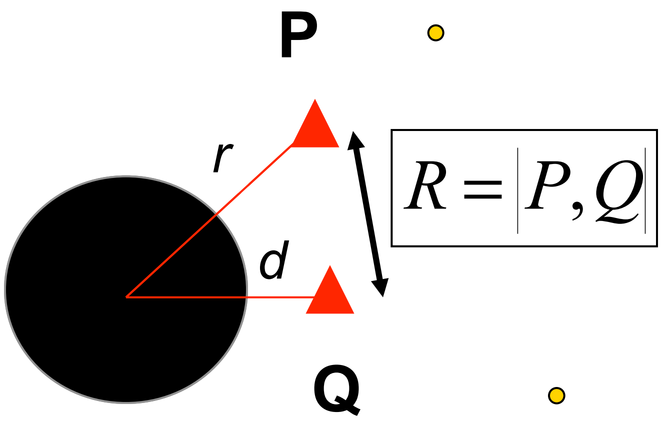

$$G_{22}(\mathbf{x},\mathbf{y};\omega) = v^0 + v^d = \frac{1}{4\mathrm{i}\mu}\left\{H_0^{(2)}(kR) + \sum_{n=0}^{\infty} \varepsilon_n A_n H_n^{(2)}(kd) H_n^{(2)}(kr)\cos n\theta\right\}.$$

$$A_n = -\frac{J_n(ka)J_n'(qa) - \xi J_n'(ka)J_n(qa)}{H_n^{(2)}(ka)J_n'(qa) - \xi H_n^{(2)\prime}(ka)J_n(qa)}. \qquad \textit{with} \qquad \xi = \frac{\mu_E k}{\mu_T q} = \frac{\rho_E \beta_E}{\rho_T \beta_T},$$

Consider an incident plane wave:

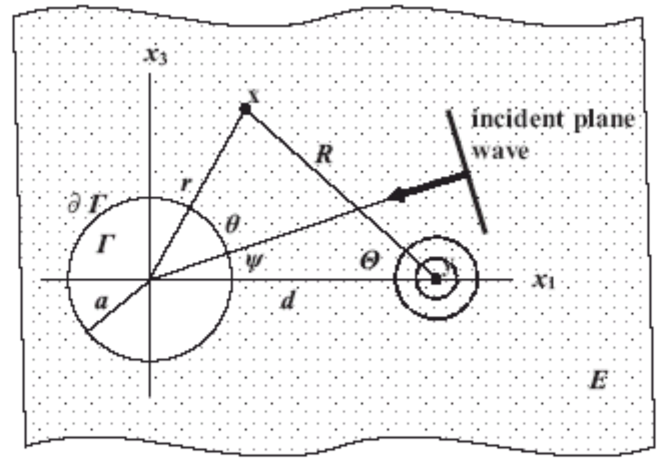

$$v(\mathbf{x},\omega,t)=F(\omega,\psi)\exp(-i\,kx_j n_j)\exp(i\,\omega t),$$

Expansion (polar coordinates):

$$v^0(\mathbf{x},\omega)=F(\omega)\sum_{n=0}^{\infty}\varepsilon_n \mathrm{i}^n J_n(kr)\cos n(\psi-\theta),\text{ and}$$

and the diffracted field

$$v^d(\mathbf{x},\omega)=F(\omega)\sum_{n=0}^{\infty}\varepsilon_n \mathrm{i}^n A_n H_n^{(2)}(kr)\cos n(\psi-\theta).$$

The incident plane wave and the diffracted field reduce to

$$v(r,\theta;\psi)=F(\omega)\sum_{n=0}^{\infty}V_n(r,\omega)\cos n(\theta-\psi),$$

where

$$V_n(r,\omega)=\mathrm{i}^n\varepsilon_n\left[J_n(kr)-A_nH_n^{(2)}(kr)\right],$$

Correlation:

$$v(\mathbf{y},\omega)v^*(\mathbf{x},\omega) = F^2(\omega)\sum_{n=0}^{\infty}\sum_{m=0}^{\infty} V_n(d,\omega)V_m^*(r,\omega)\cos n\psi \cos m(\psi-\theta)$$

azimuthal average:equipartition of the incident field

$$\langle v(\mathbf{y},\omega)v^*(\mathbf{x},\omega)\rangle = F^2(\omega)\sum_{m=0}^{\infty}\frac{1}{\varepsilon_m}V_m(d,\omega)V_m^*(r,\omega)\cos m\theta$$

$$\frac{1}{\varepsilon_m}V_m(d,\omega)V_m^*(r,\omega) = \frac{\varepsilon_m}{D_m^2}(N_m Y_m(kd) - M_m J_m(kd))(N_m Y_m(kr) - M_m J_m(kr))$$

Noting that:

$$\mathrm{Im}[G_{22}(\mathbf{x},\mathbf{y};\omega)] = \frac{-1}{4\mu}\sum_{m=0}^{\infty}\frac{\varepsilon_m}{D_m^2}(N_m Y_m(kd) - M_m J_m(kd))(N_m Y_m(kr) - M_m J_m(kr))\cos m\theta$$

the exact relation:

$$\langle v(\mathbf{y},\omega)v^*(\mathbf{x},\omega)\rangle = -8E_{SH}k^{-2}\,\mathrm{Im}[G_{22}(\mathbf{x},\mathbf{y},\omega)].$$

including near filed, scattering, resonances,…..

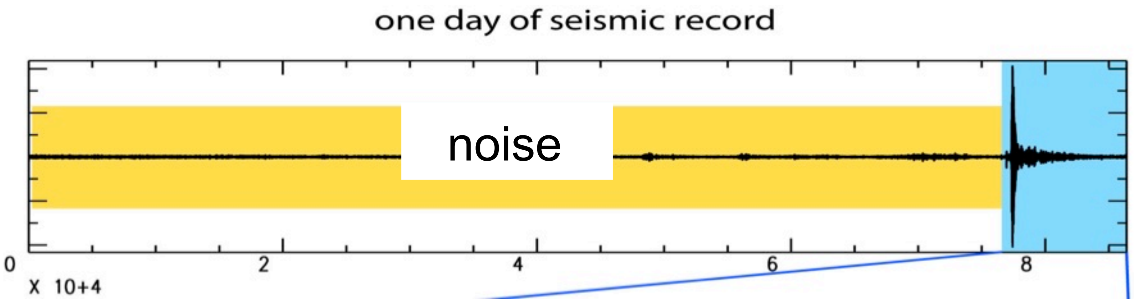

Networks with continuous recording = huge amount of noise data!

Measurement Method Applied to a Pair of North American Stations

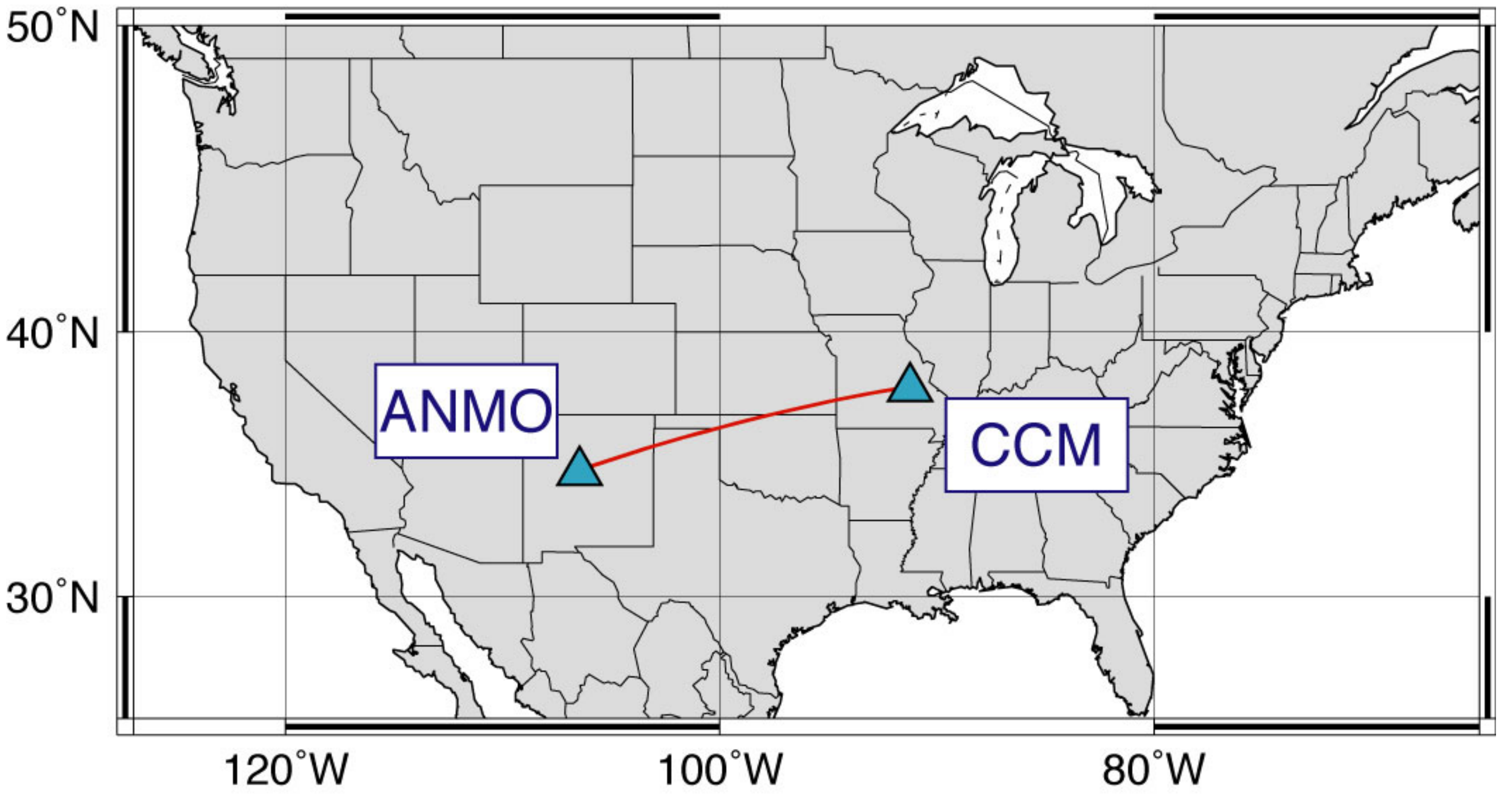

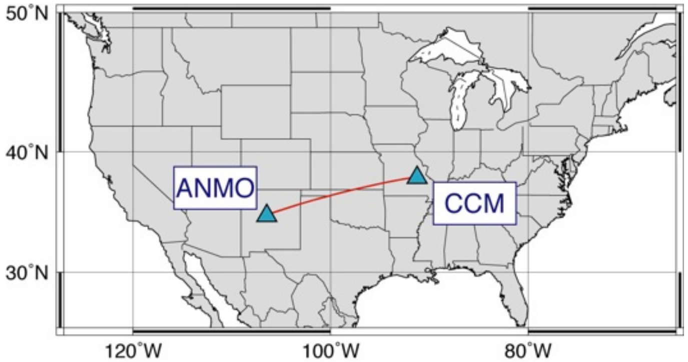
50˚N
40˚N
30˚N
120˚W
100˚W
80˚W
ANMO
CCM

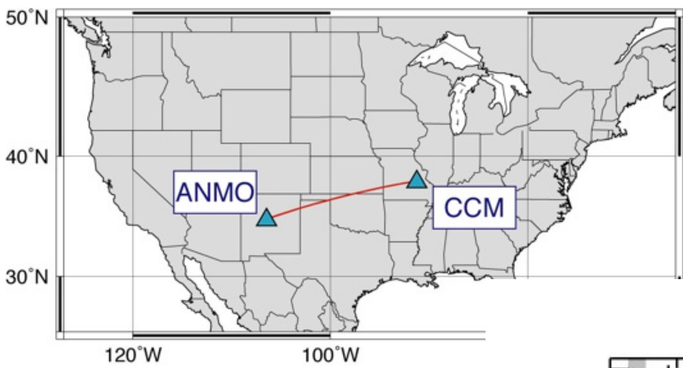

1. Raw data (January 18, 2002)

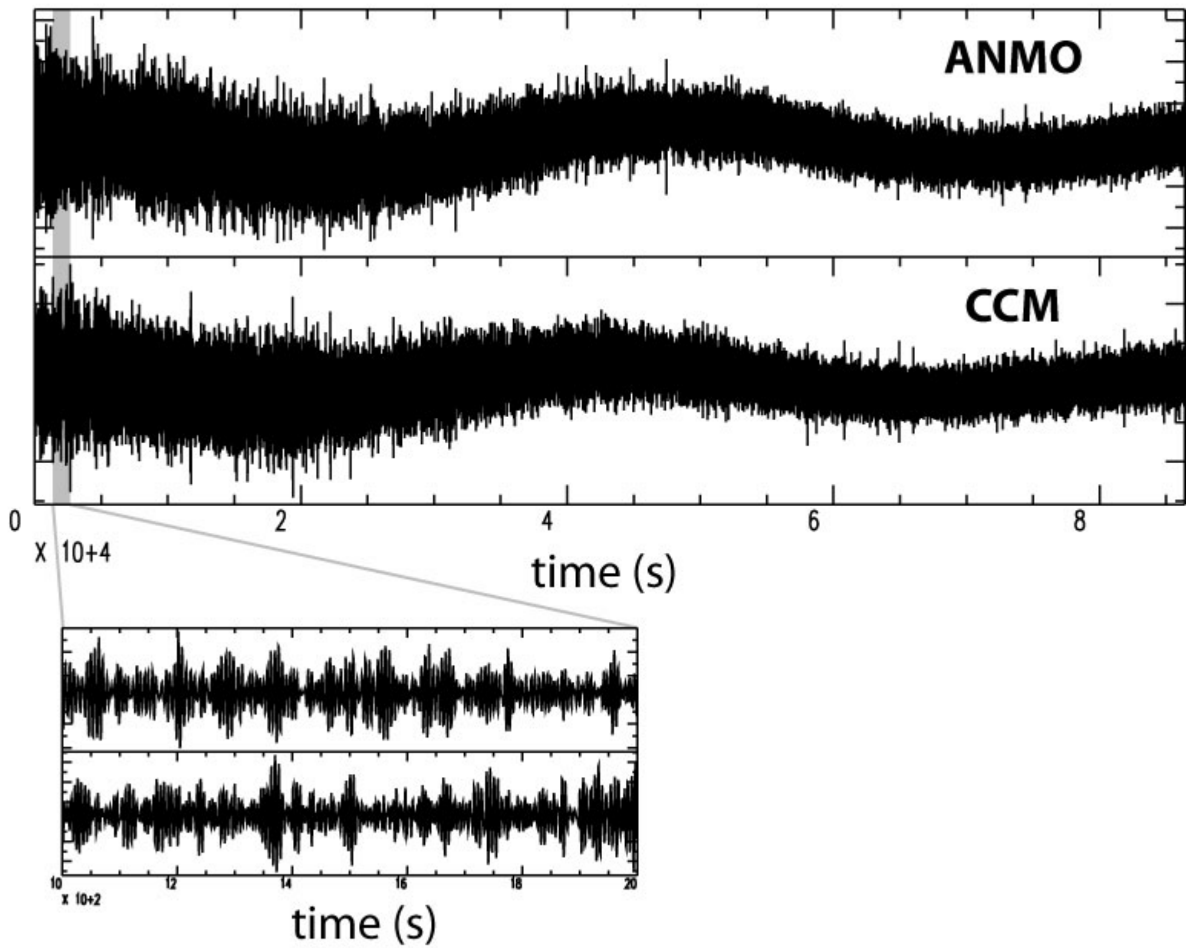

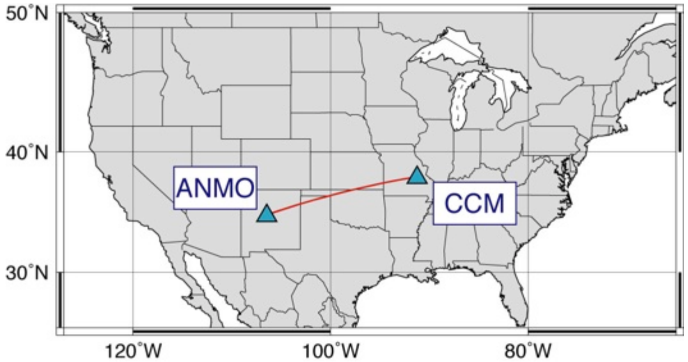

1. Raw data (January 18, 2002)

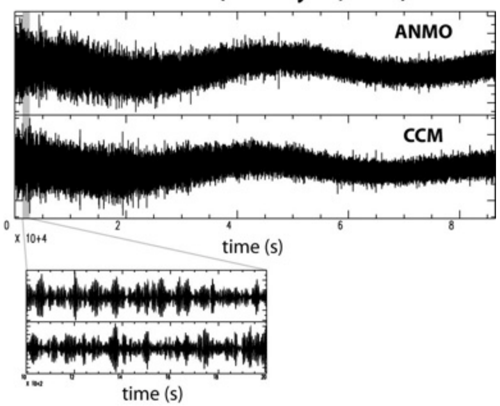

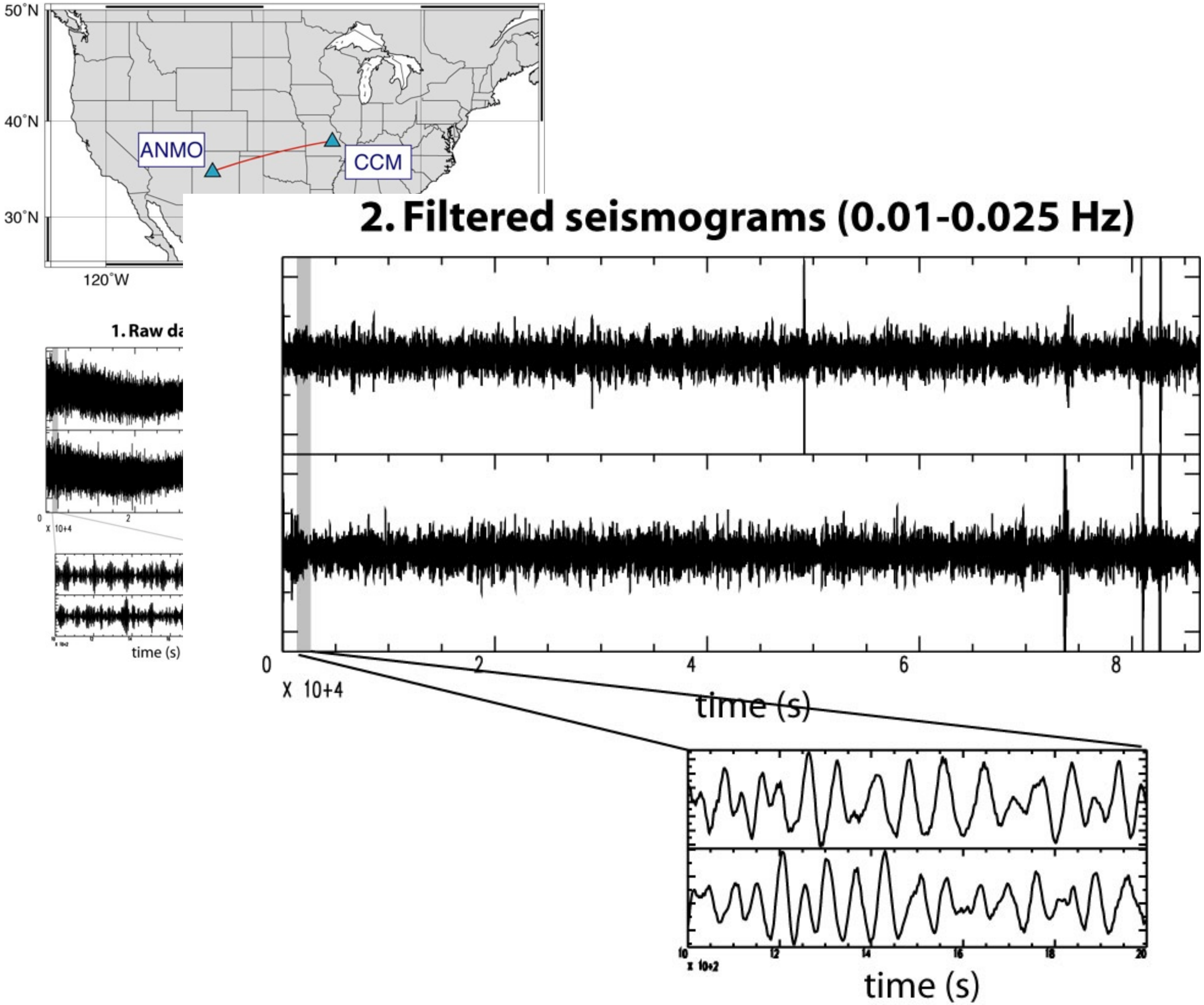

50°N
40°N
30°N
120°W
ANMO
CCM
1. Raw da
time (s)
2. Filtered seismograms (0.01-0.025 Hz)
0
2
4
6
8
X 10+4
time (s)
time (s)

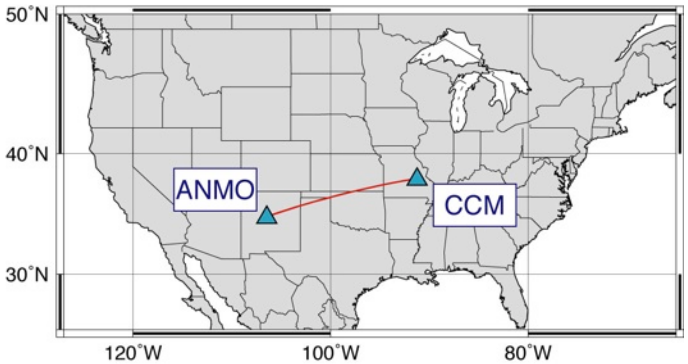

1. Raw data (January 18, 2002)

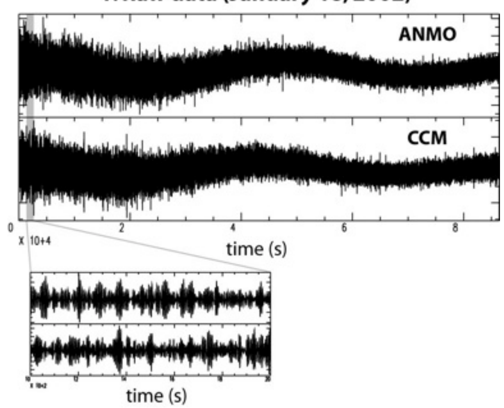

2. Filtered seismograms (0.01-0.025 Hz)

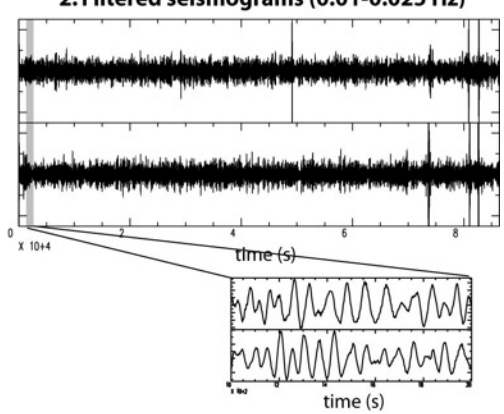

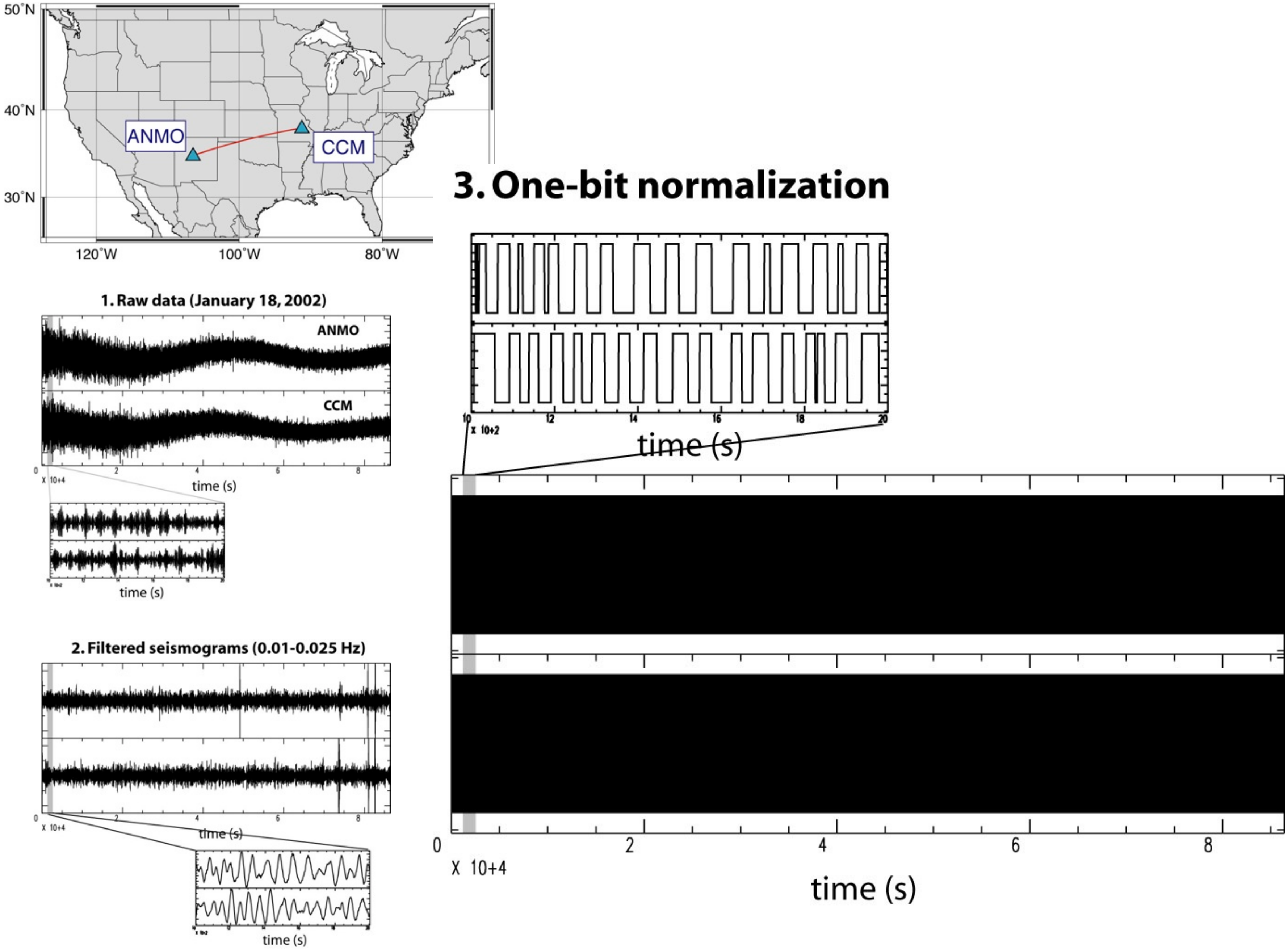
50°N
40°N
30°N
120°W
100°W
80°W
ANMO
CCM
1. Raw data (January 18, 2002)
ANMO
CCM
time (s)
time (s)
2. Filtered seismograms (0.01-0.025 Hz)
time (s)
time (s)
3. One-bit normalization
time (s)
0
2
4
6
8
X 10+4
time (s)

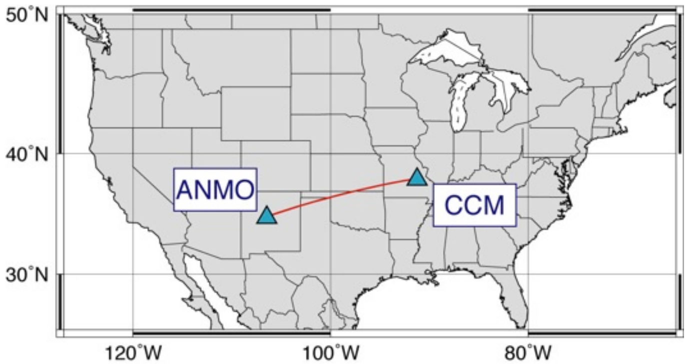

1. Raw data (January 18, 2002)

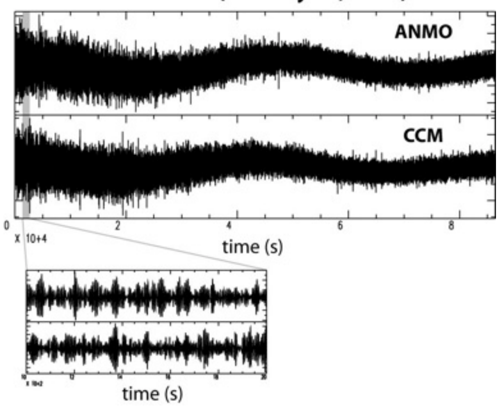

2. Filtered seismograms (0.01-0.025 Hz)

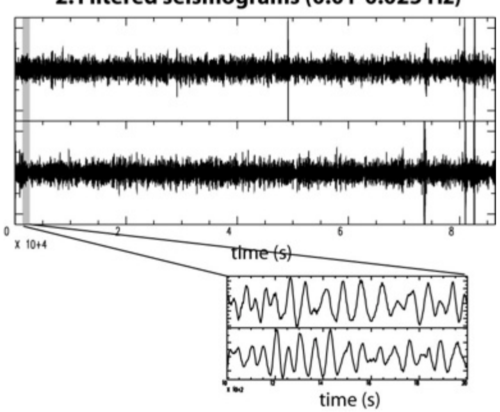

3. One-bit normalization

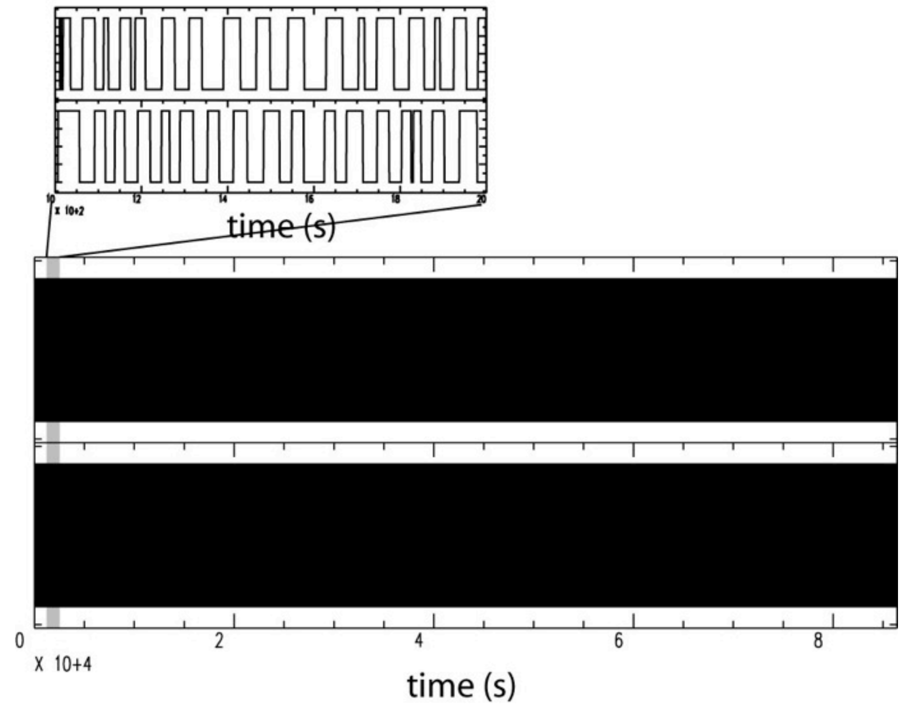

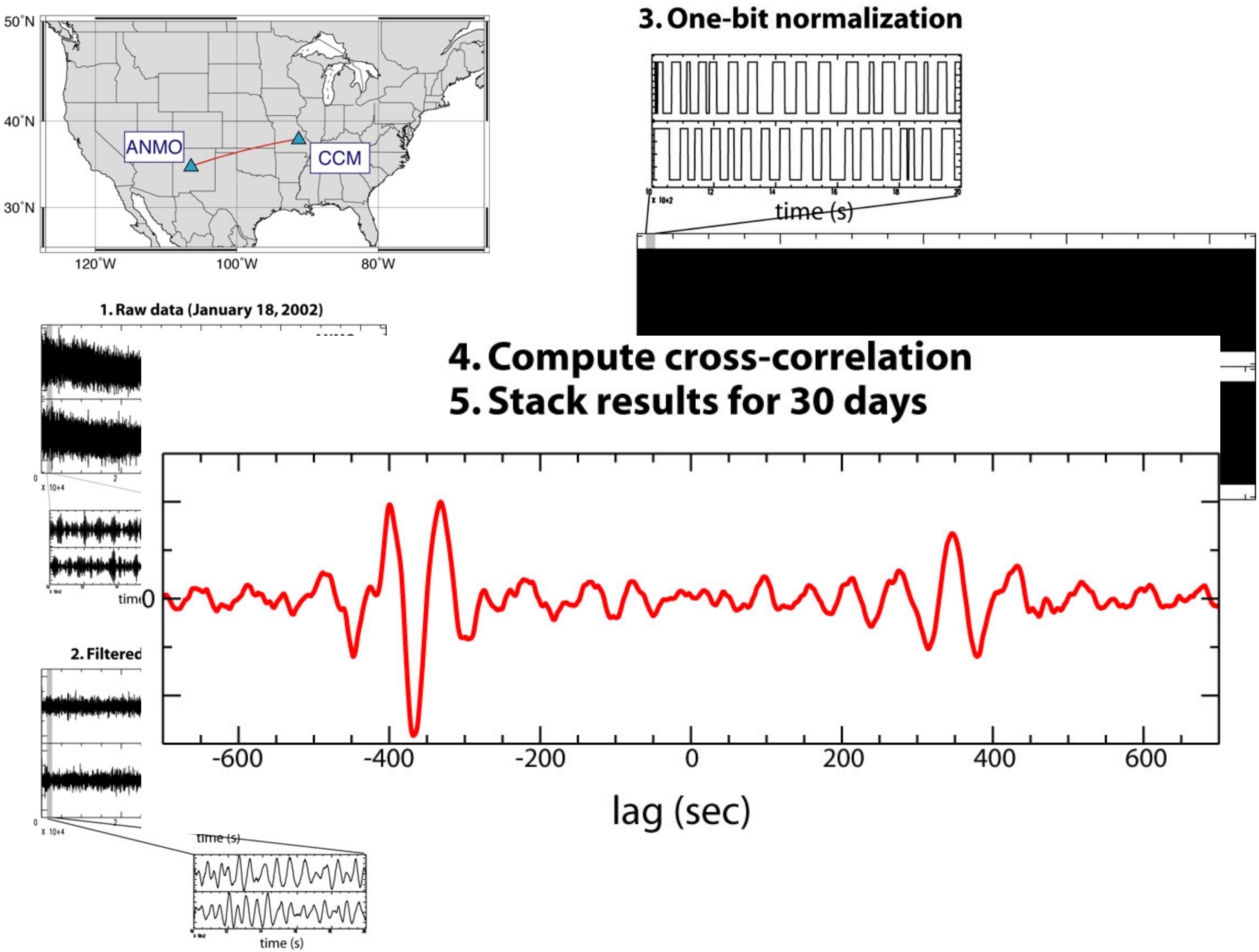
50°N
40°N
30°N
120°W
100°W
80°W
ANMO
CCM
1. Raw data (January 18, 2002)
2. Filtered
3. One-bit normalization
time (s)
4. Compute cross-correlation
5. Stack results for 30 days
0
-600
-400
-200
0
200
400
600
lag (sec)
time (s)

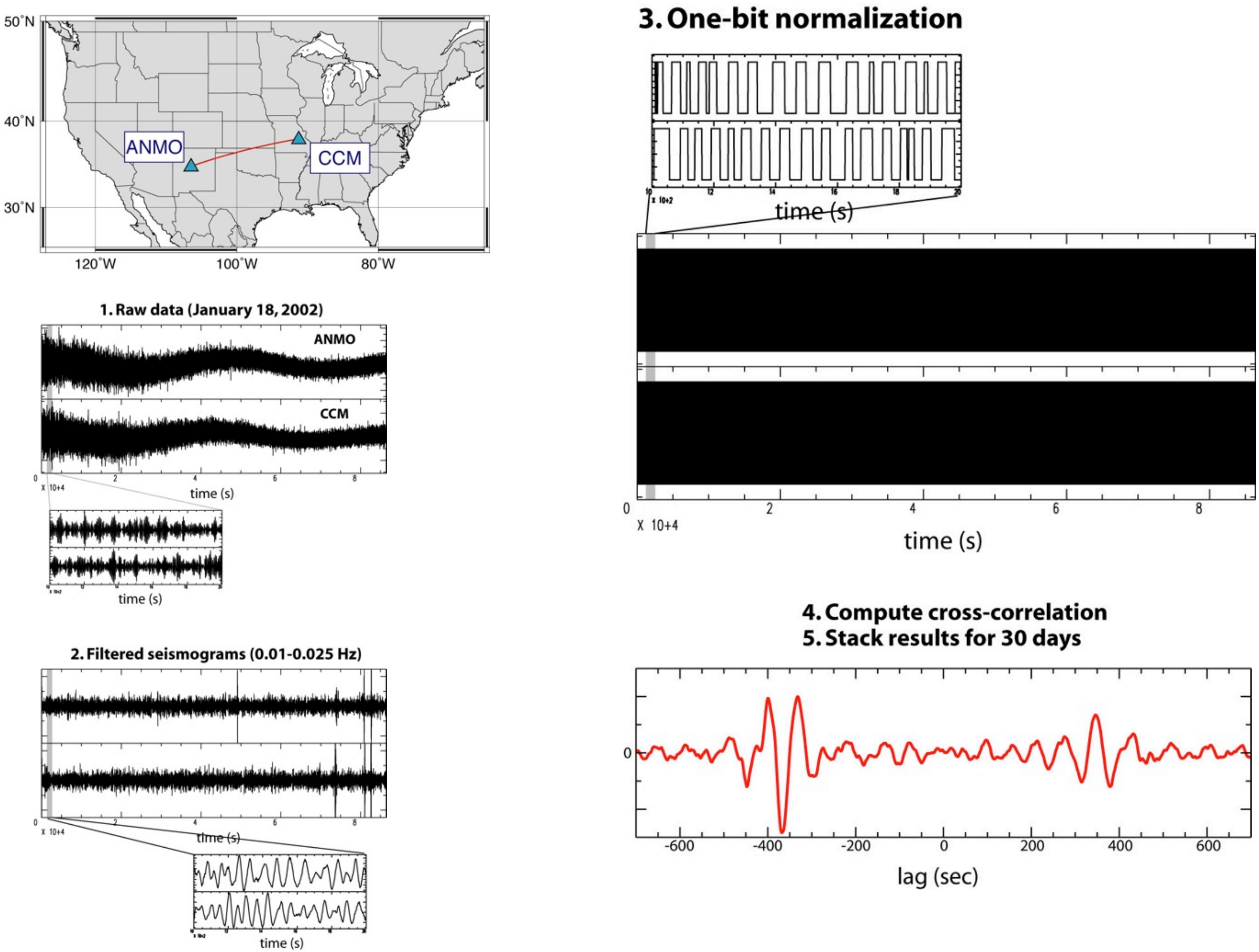
50°N
40°N
30°N
120°W
100°W
80°W
ANMO
CCM
1. Raw data (January 18, 2002)
ANMO
CCM
time (s)
time (s)
2. Filtered seismograms (0.01-0.025 Hz)
time (s)
time (s)
3. One-bit normalization
time (s)
time (s)
4. Compute cross-correlation
5. Stack results for 30 days
lag (sec)

Cross-correlations of seismic noise: ANMO - CCM

(from Shapiro and Campillo, GRL, 2004)

30 days of vertical motion

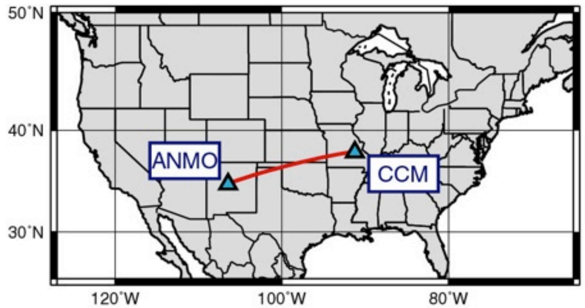

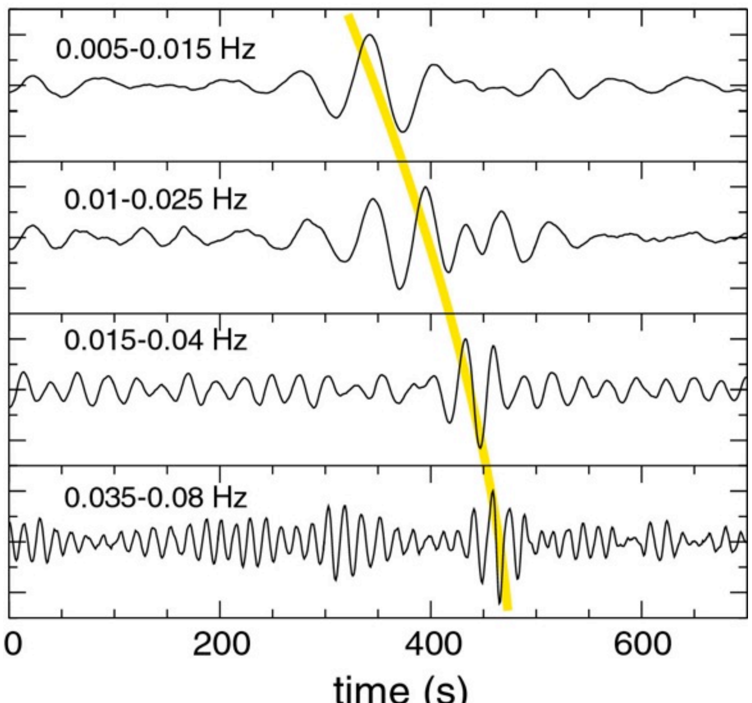

Dispersion analysis

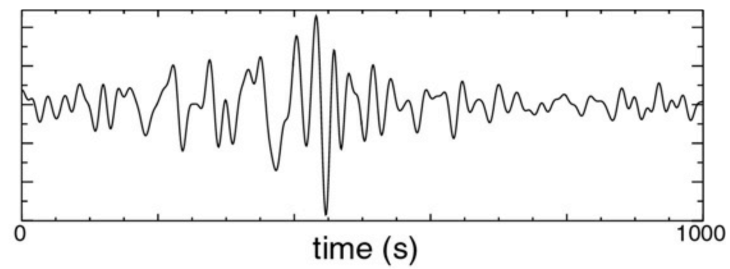

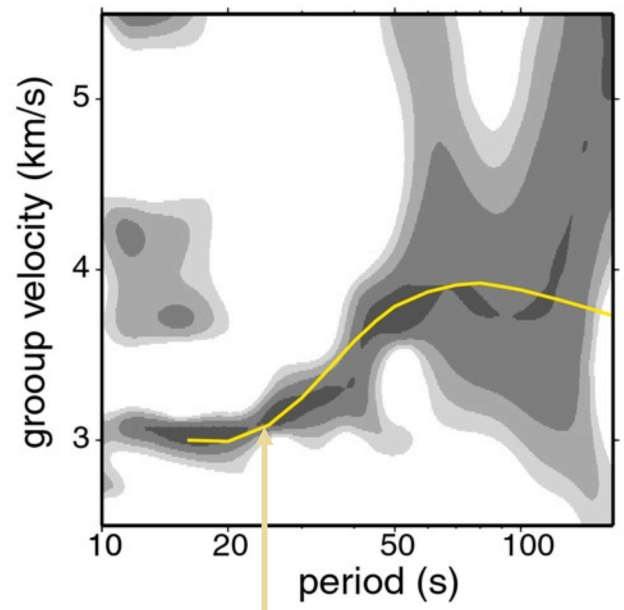

global model by Ritzwoller et al. 2002

Comparison between measured actual Green function and reconstruction

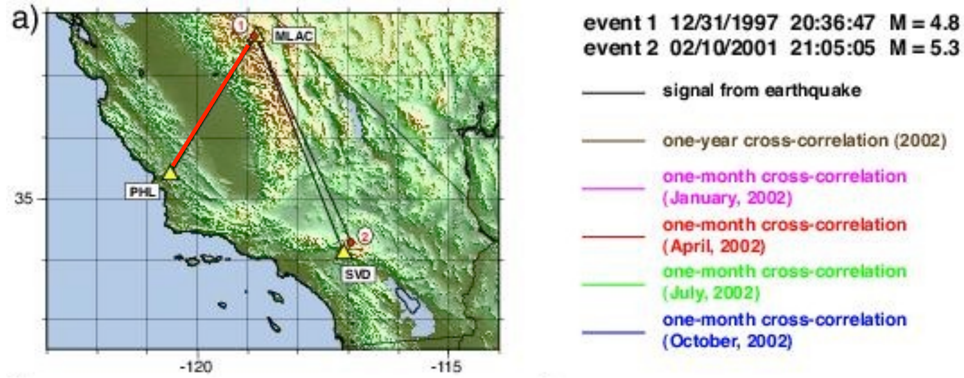

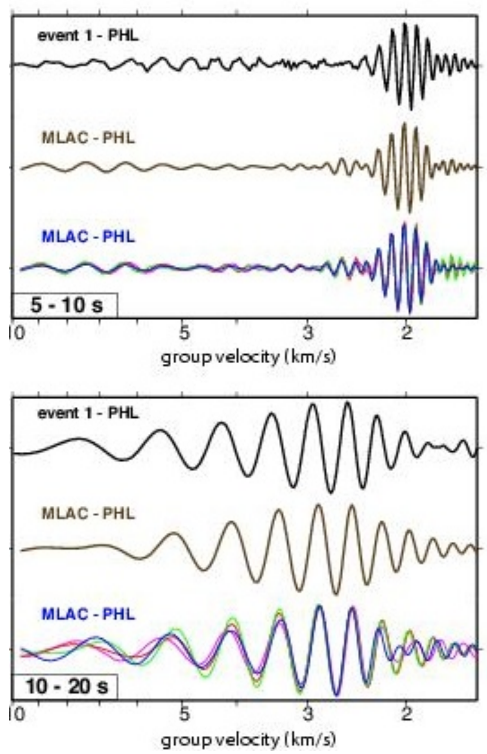

Shapiro, Campillo, Stehly et Ritzwoller, 2005

Origin of the seismic noise

Isotropic distribution of sources: symmetric cross-correlation

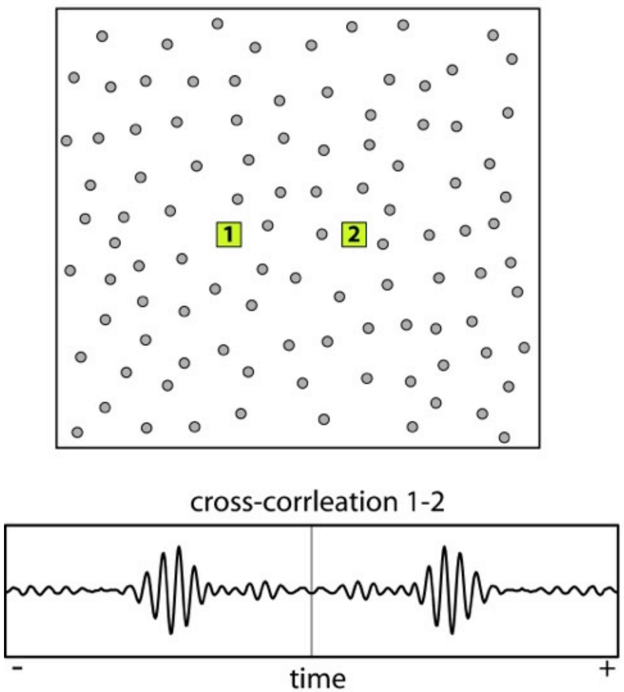

Anisotropic distribution of sources: asymmetric cross-correlation

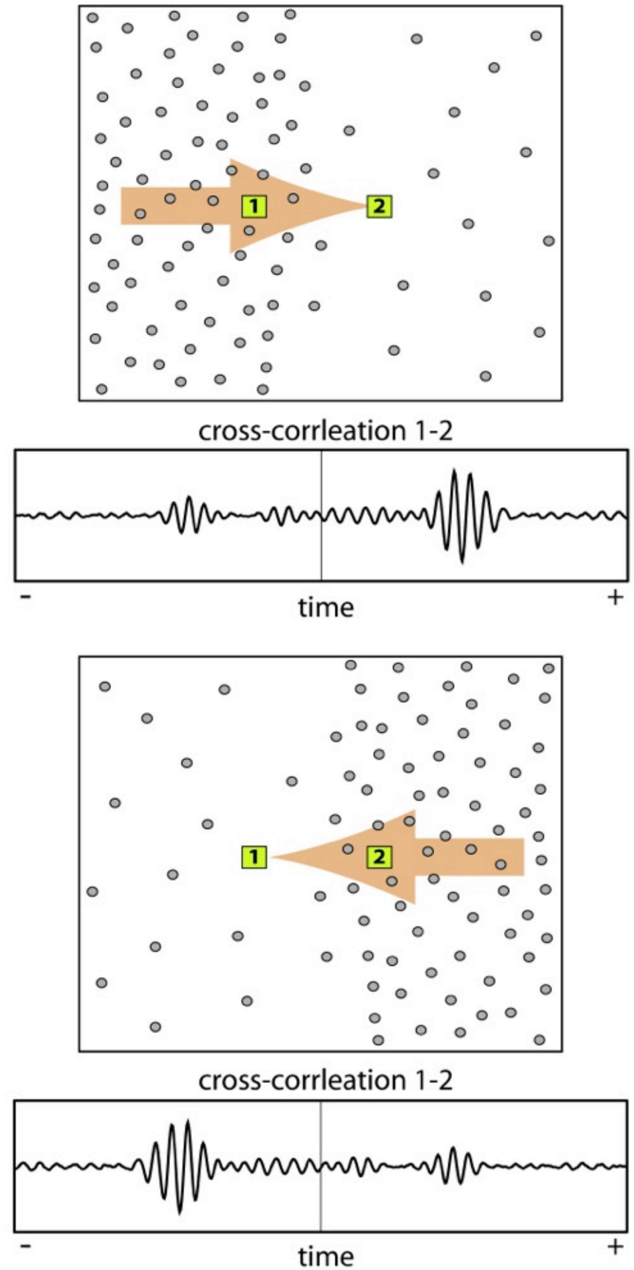

Tracking the origin of the seismic noise

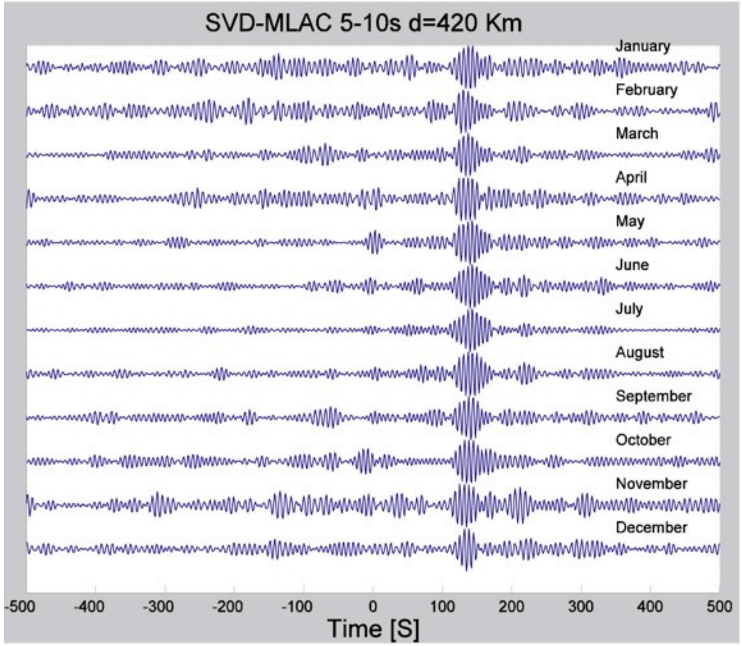

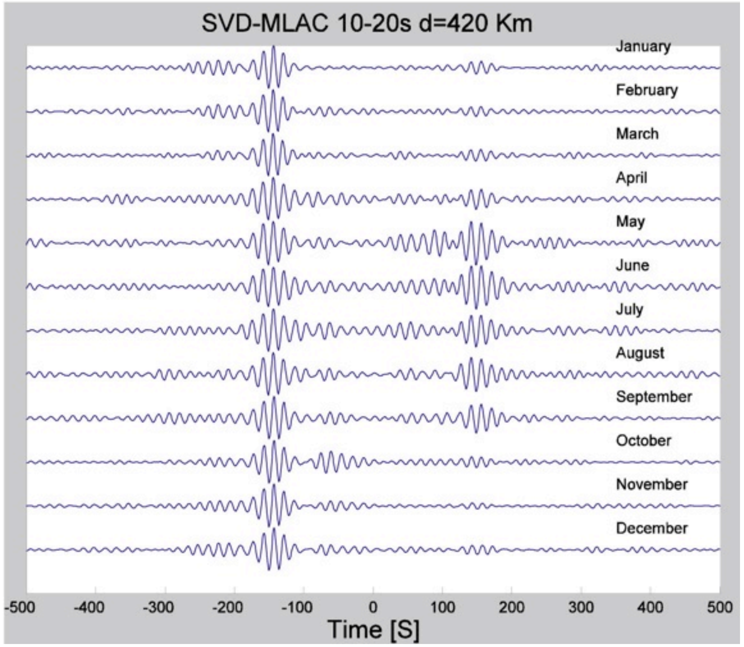

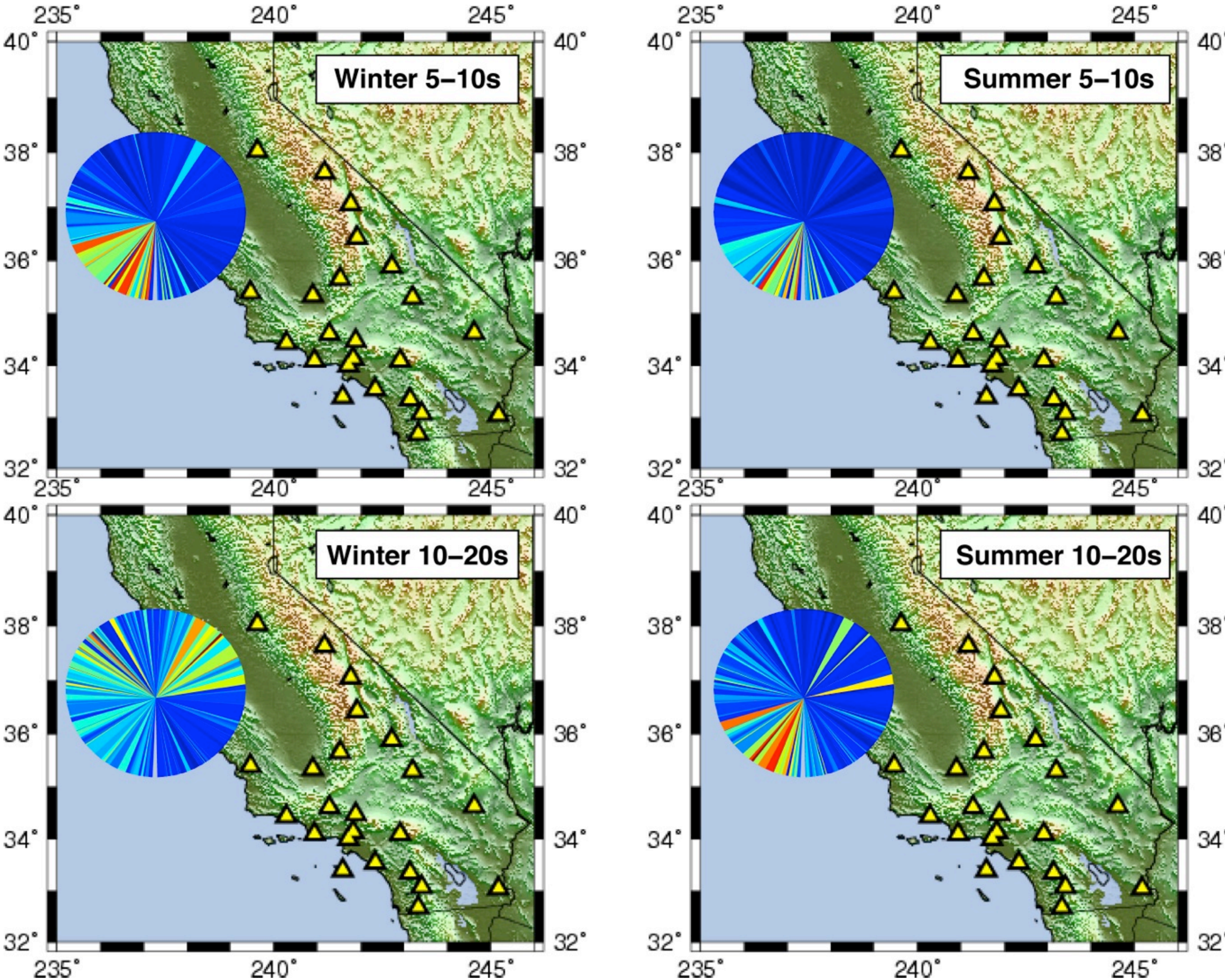
Winter 5–10s
Summer 5–10s
Winter 10–20s
Summer 10–20s
235°
240°
245°
32°
34°
36°
38°
40°

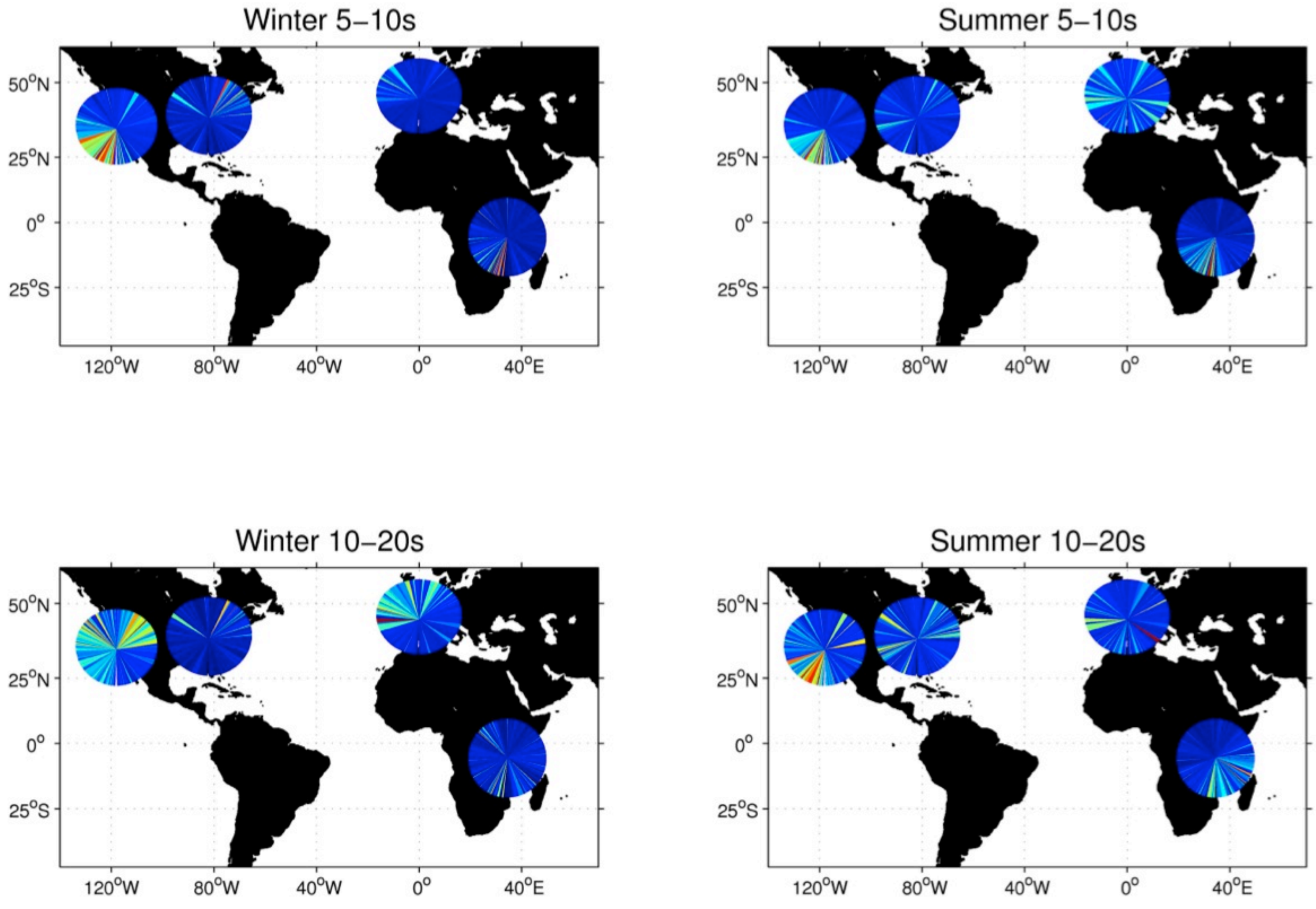

Winter 5−10s
Summer 5−10s
Winter 10−20s
Summer 10−20s
50°N
25°N
0°
25°S
120°W
80°W
40°W
0°
40°E

Apparent origin of the noise

Average sea wave height

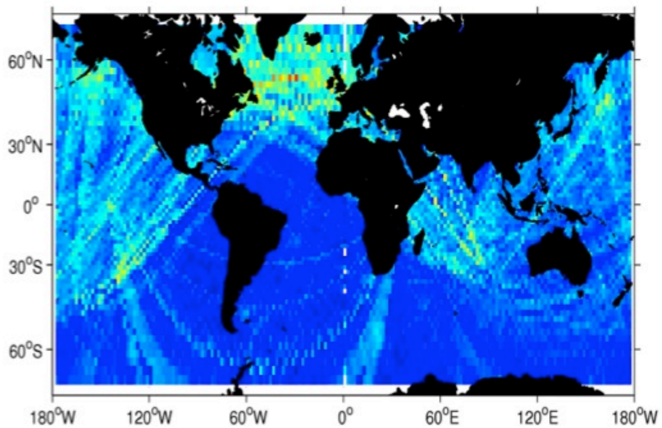

winter

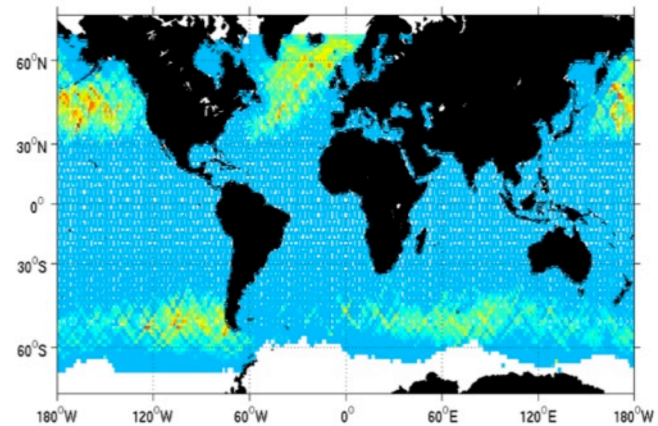

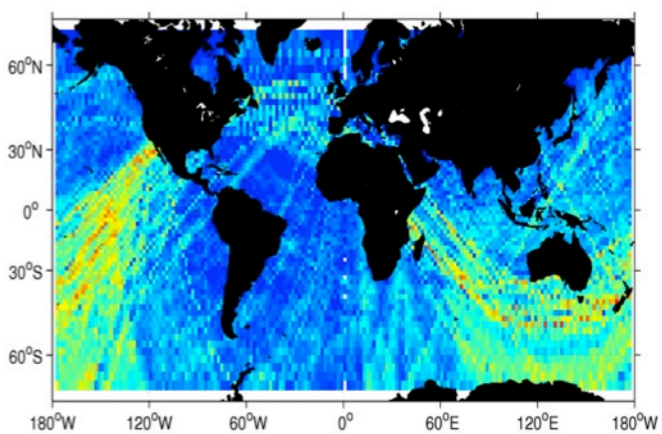

summer

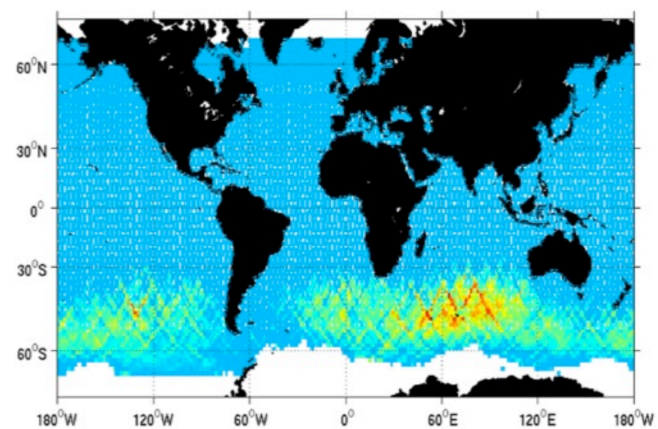

Imaging California with earthquake data

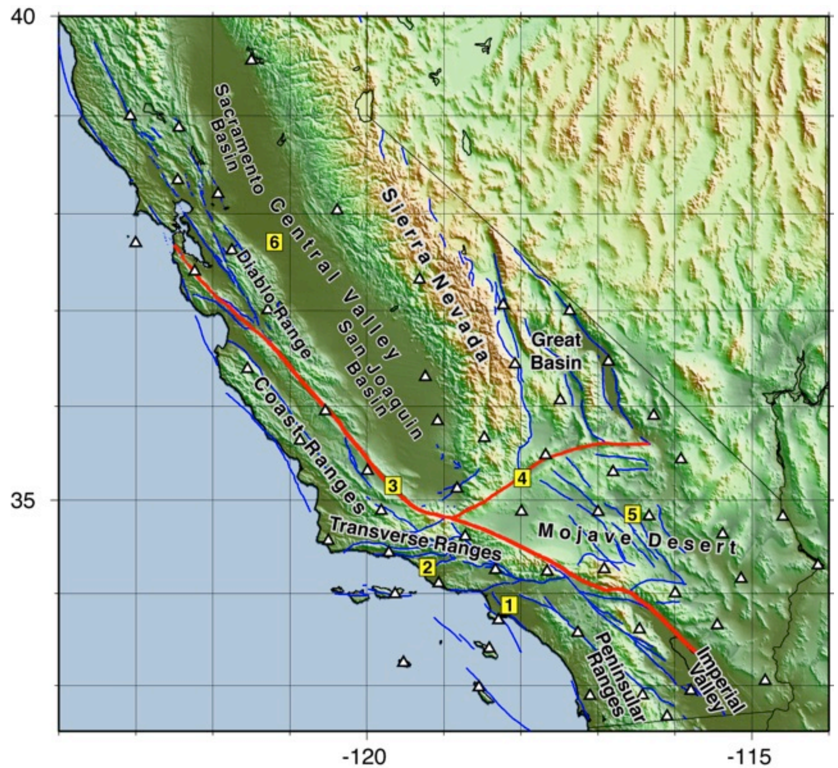

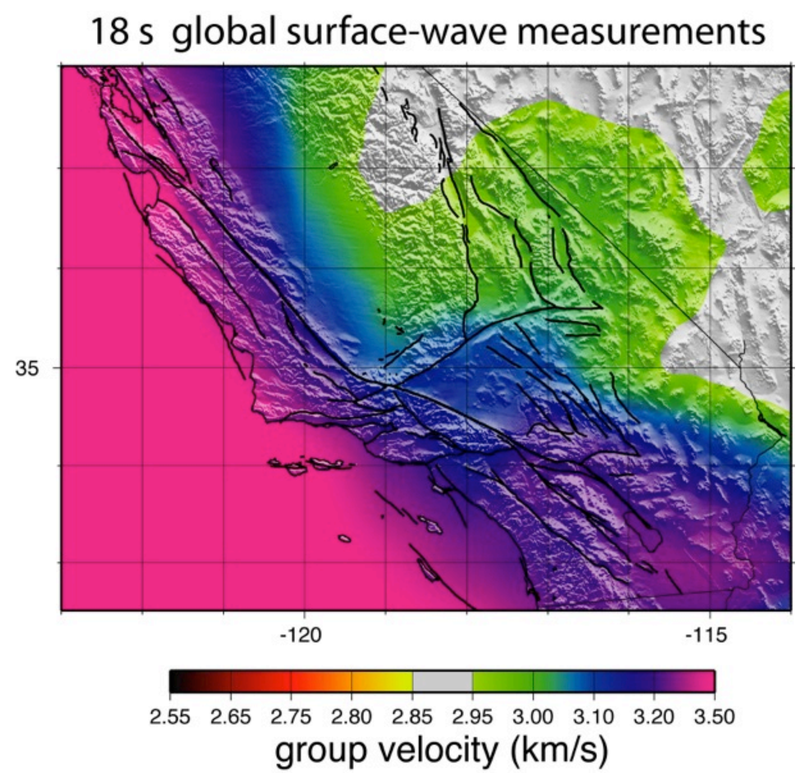

Trajets déduits du bruit (~3000 paires)

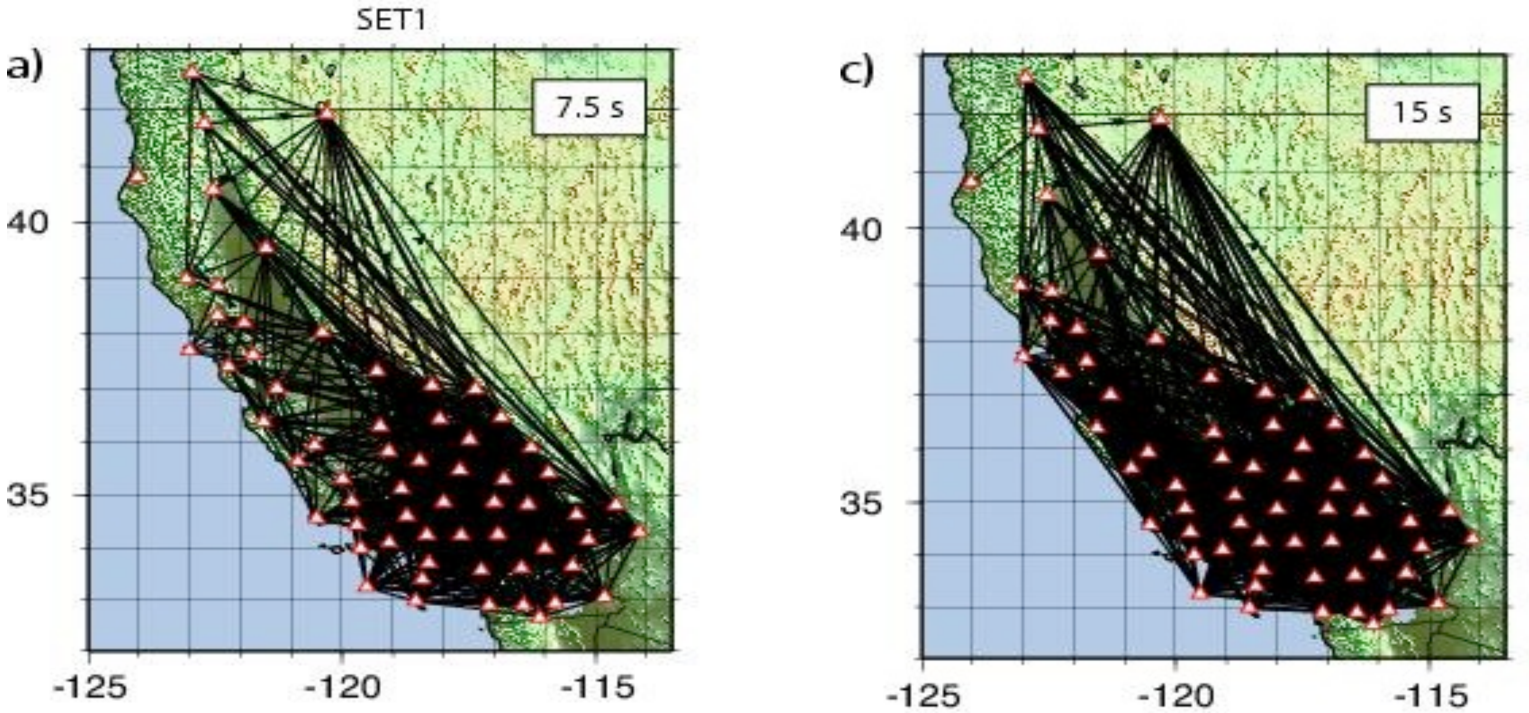

High resolution velocity map obtained from noise (Rayleigh 7.5 s)

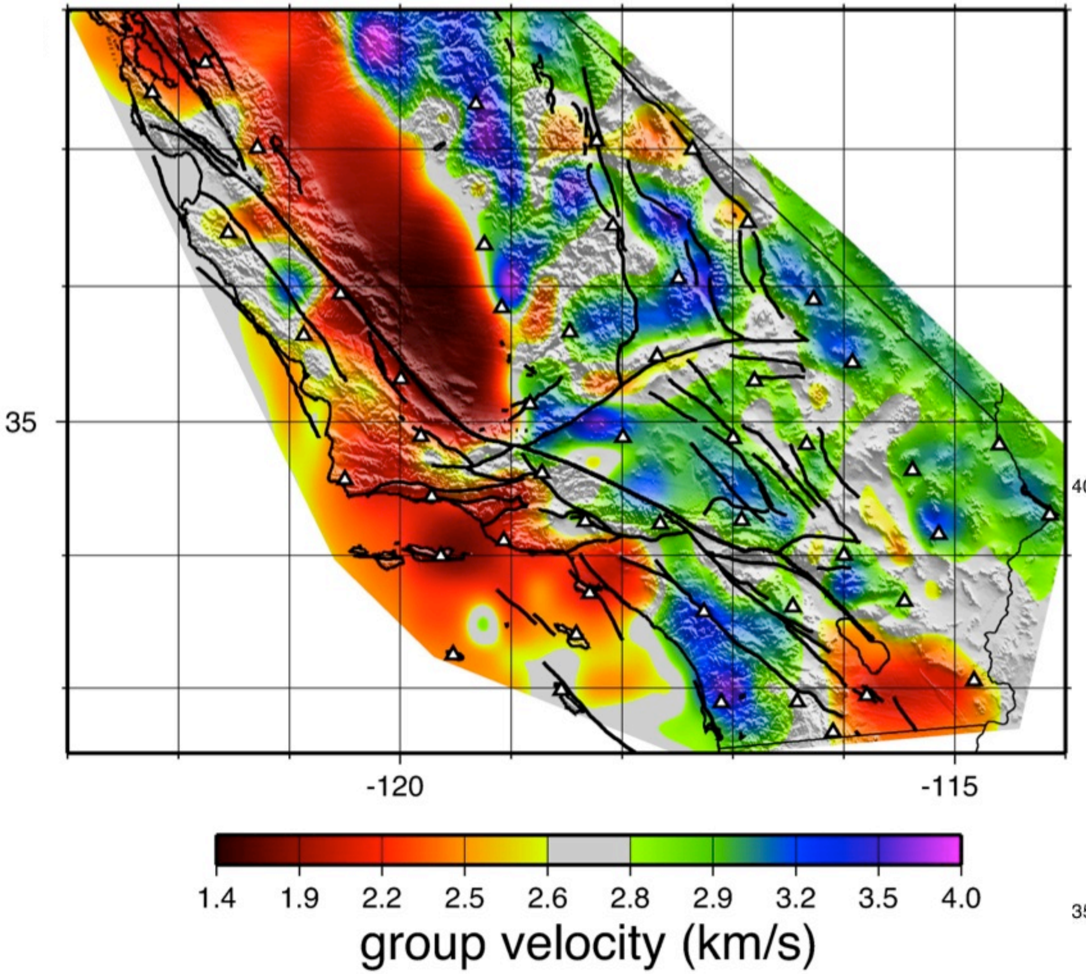

Main geological features

Shapiro, Campillo, Stehly et Ritzwoller, 2005

High resolution velocity map obtained from noise (Rayleigh 7.5 s)

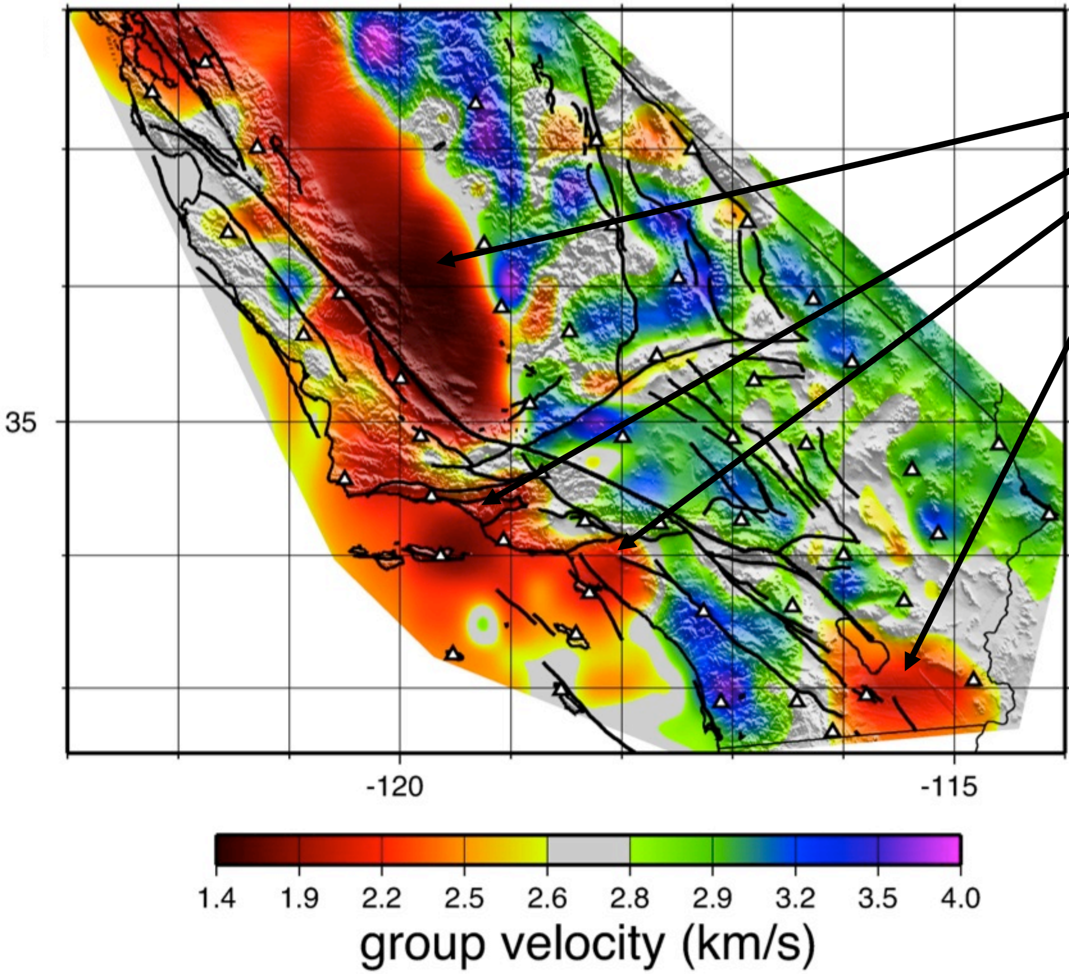

Sedimentary basins
(➔S wave velocity)

Main geological features

High resolution velocity map obtained from noise (Rayleigh 7.5 s)

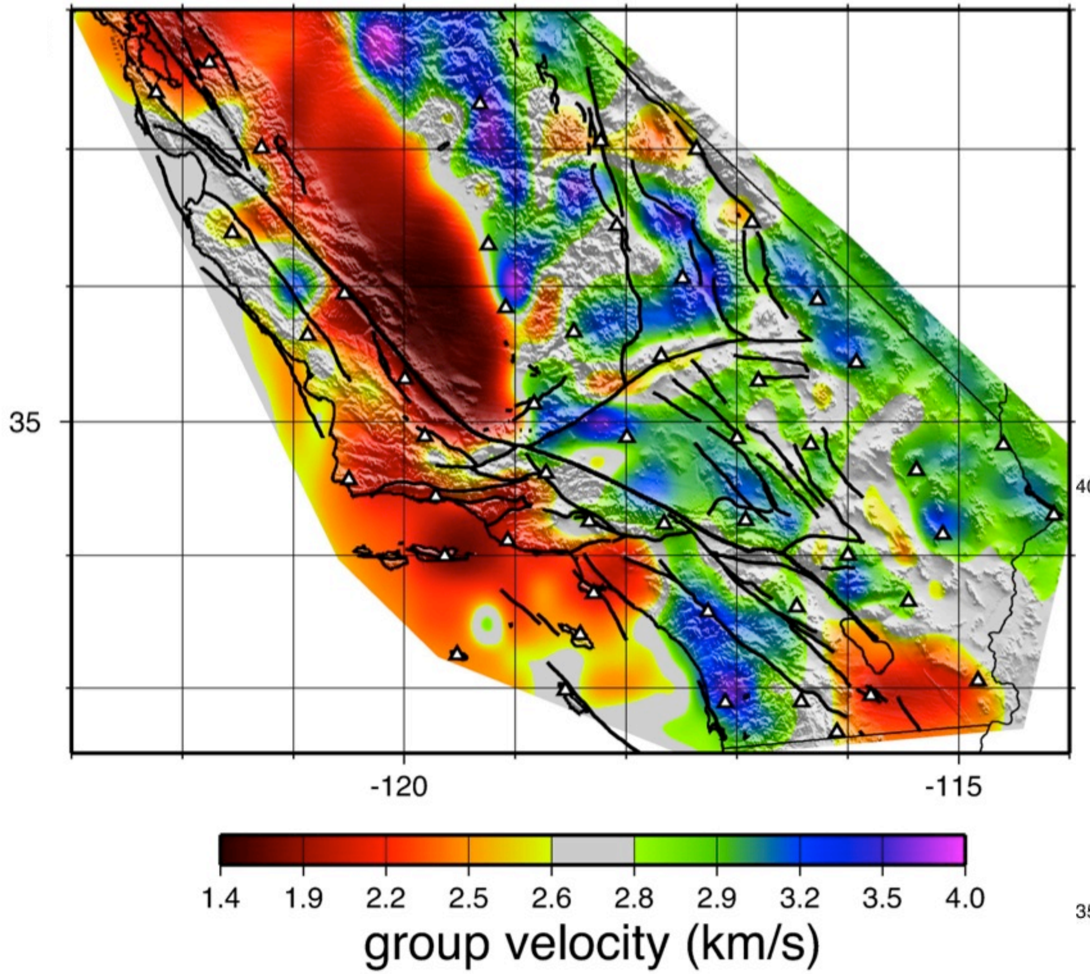

Main geological features

High resolution velocity map obtained from noise (Rayleigh 15 s ~ middle crust)

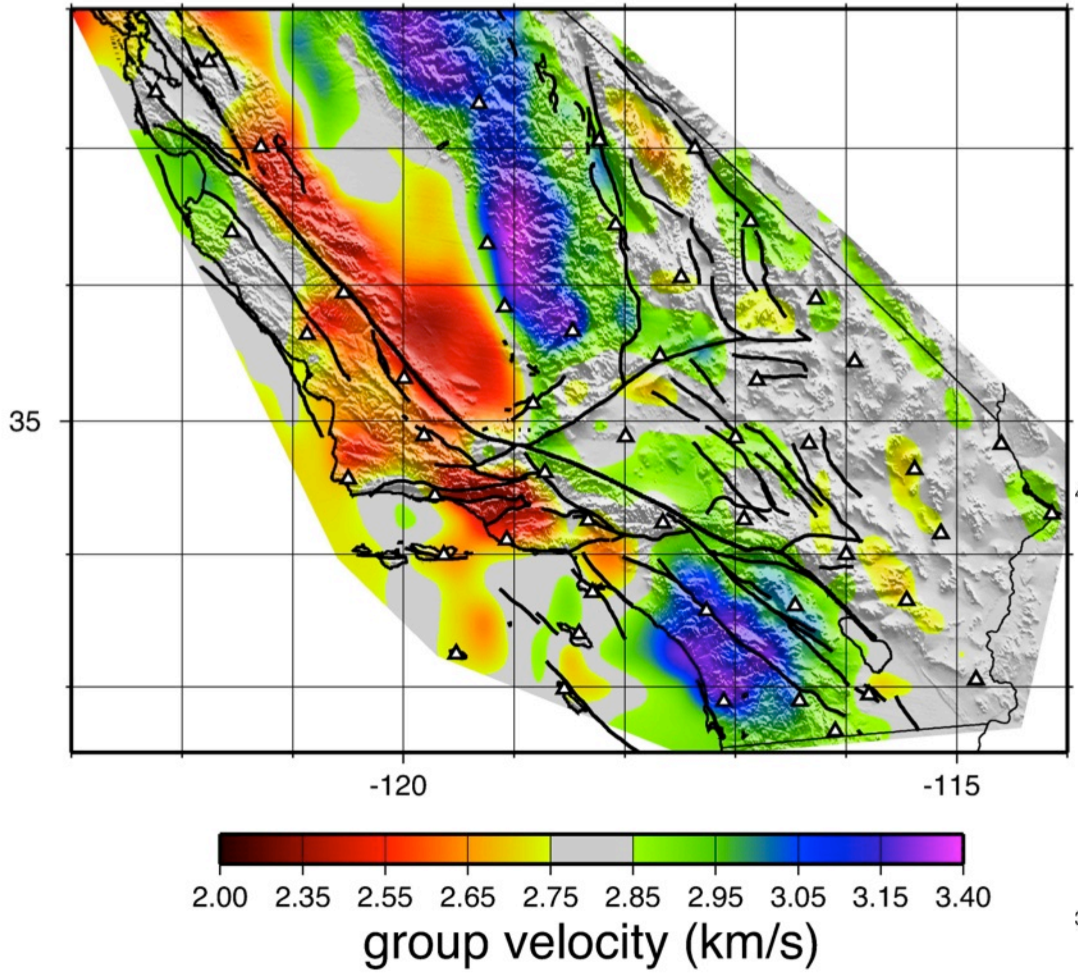

Main geological features

High resolution velocity map obtained from noise (Rayleigh 15 s ~ middle crust)

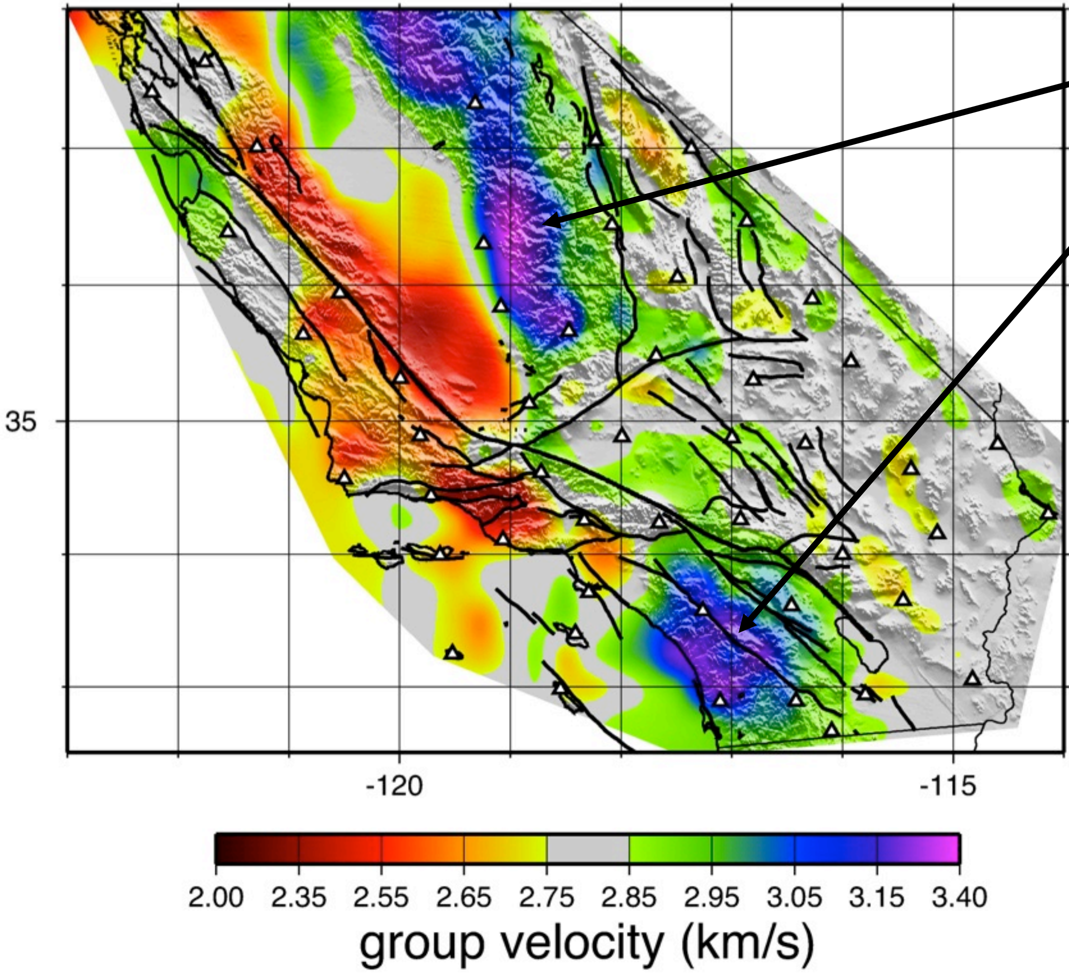

Granitic batholiths

Main geological features

High resolution velocity map obtained from noise (Rayleigh 15 s ~ middle crust)

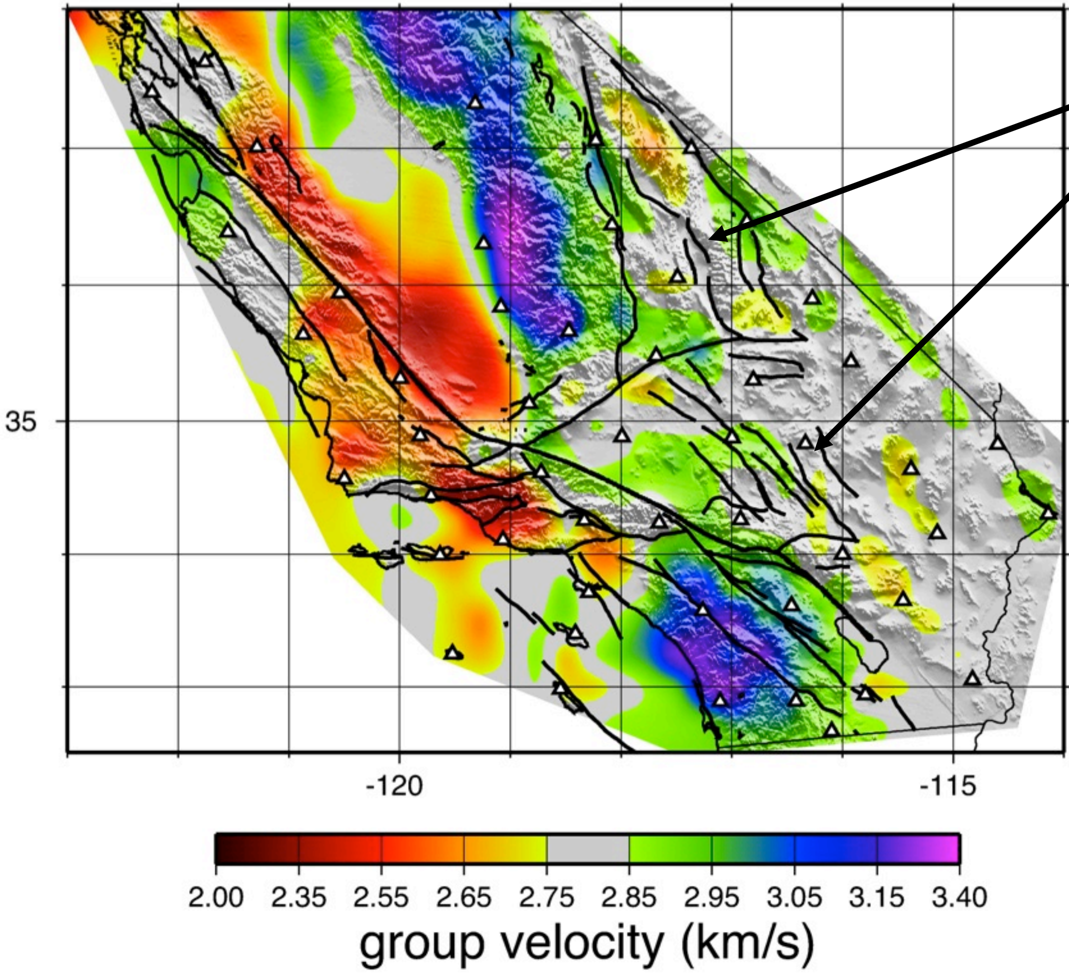

Great basin and Mojave

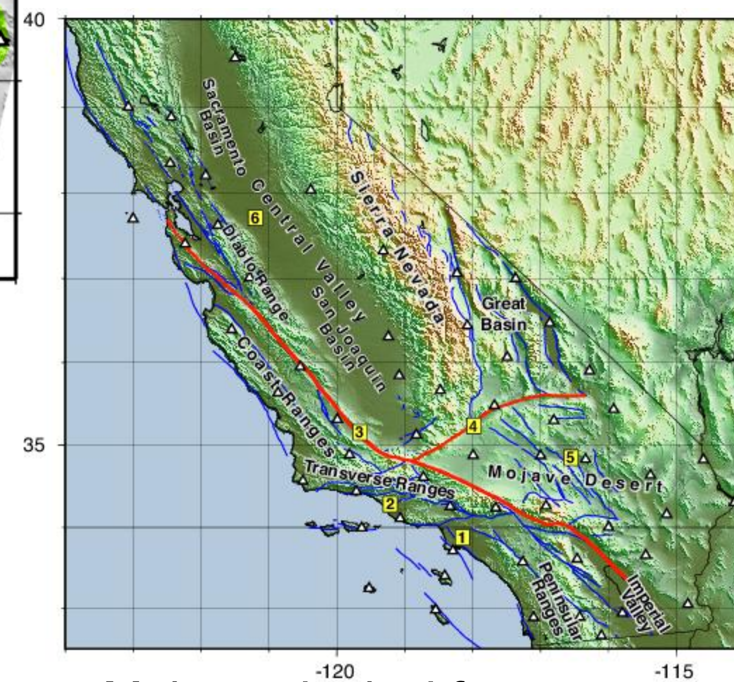

Main geological features

High resolution velocity map obtained from noise (Rayleigh 15 s ~ middle crust)

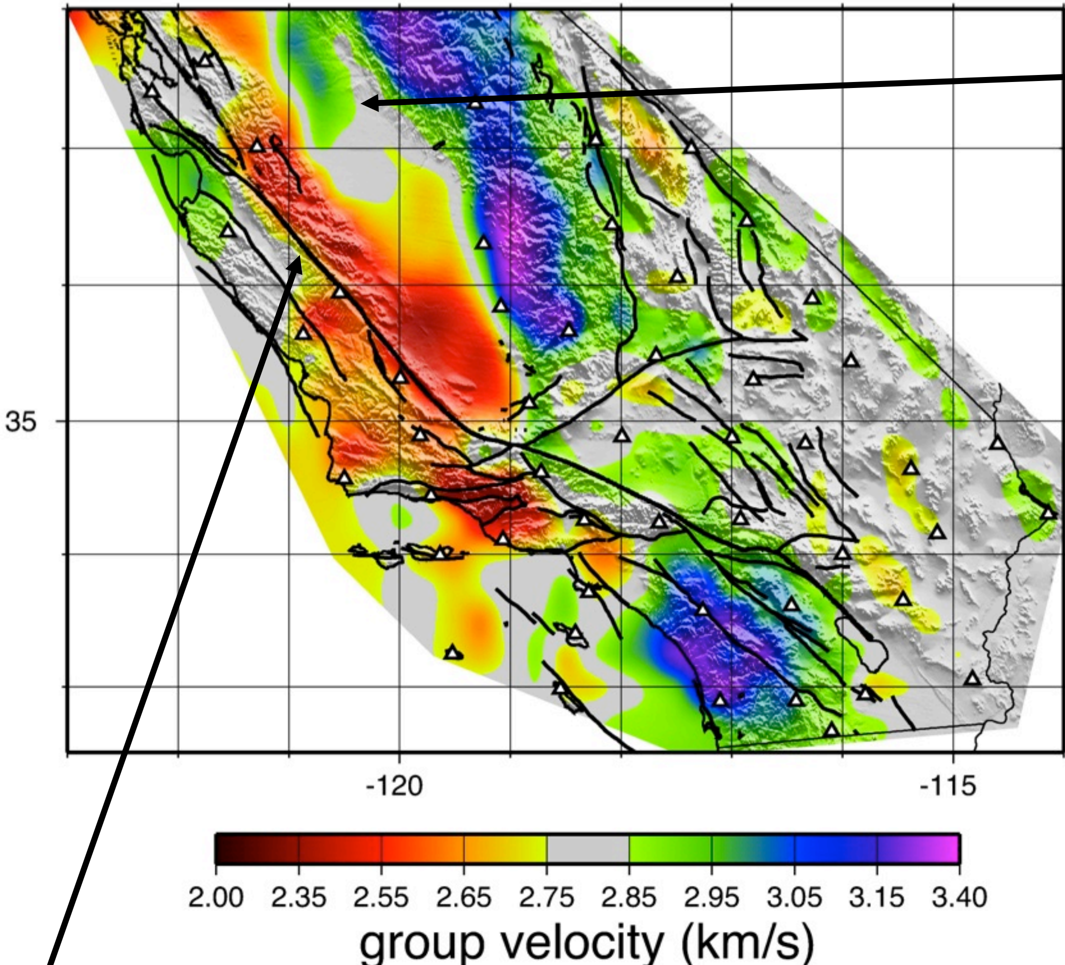

Stockton Arch

SAF

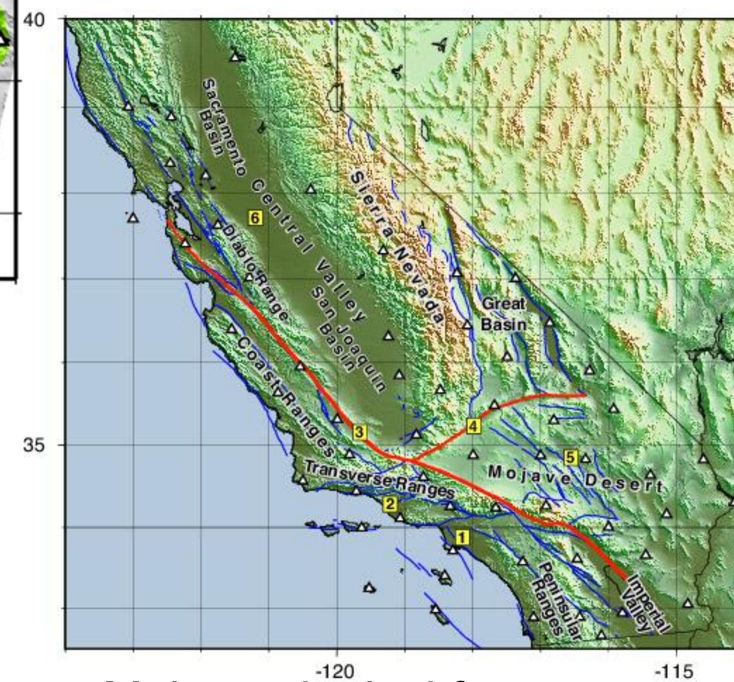

Main geological features

Comparison noise correlation vs earthquake data

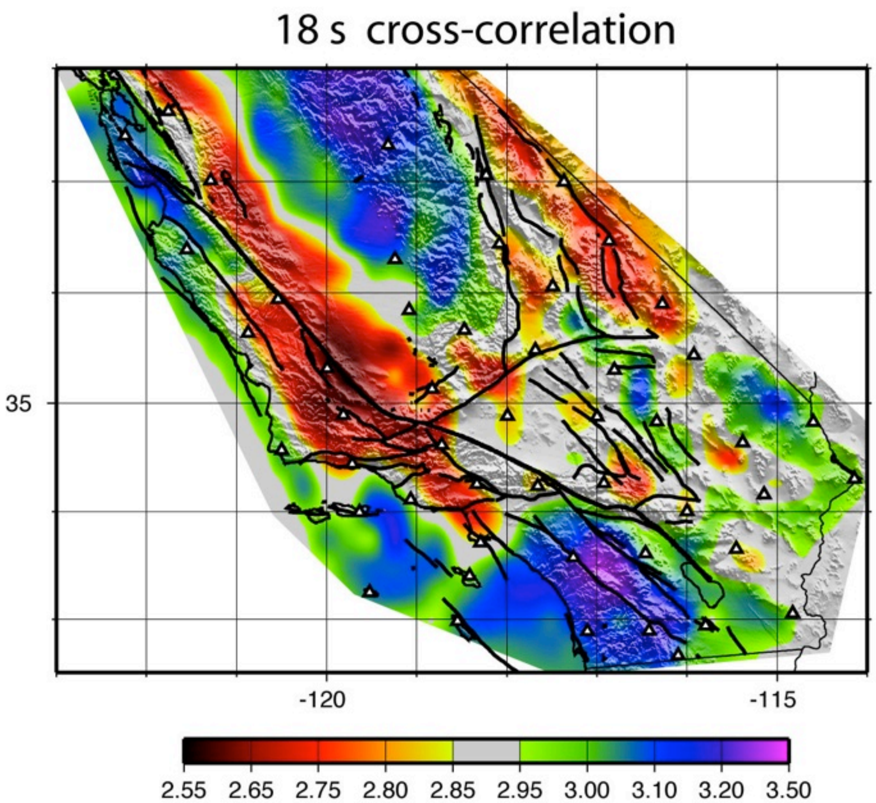

Vitesse des ondes de Rayleigh

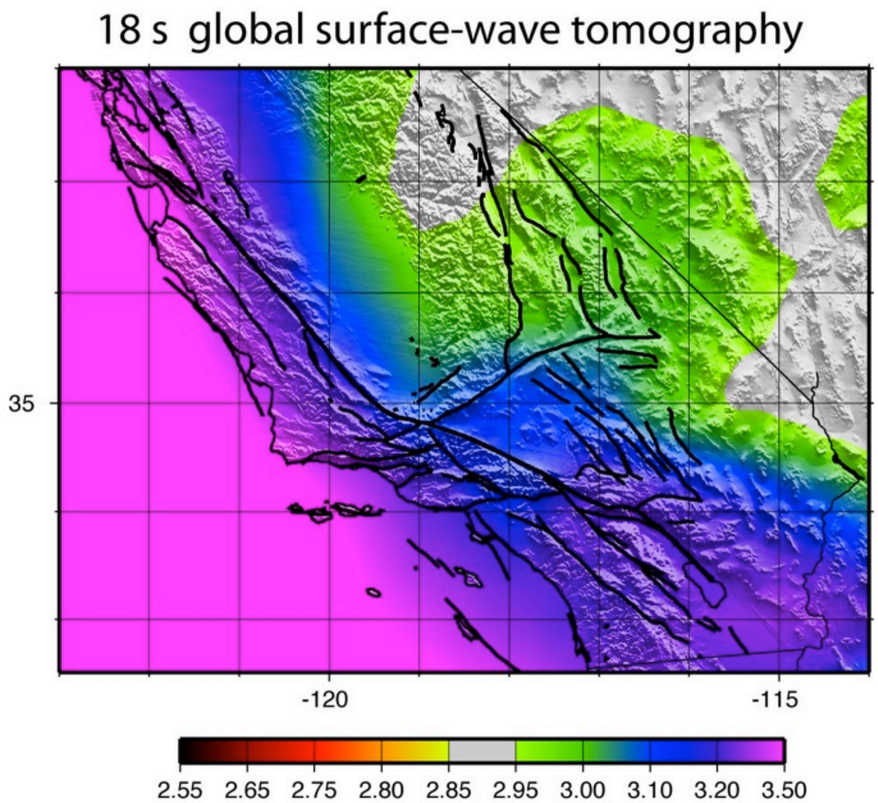

Vitesse des ondes de Rayleigh

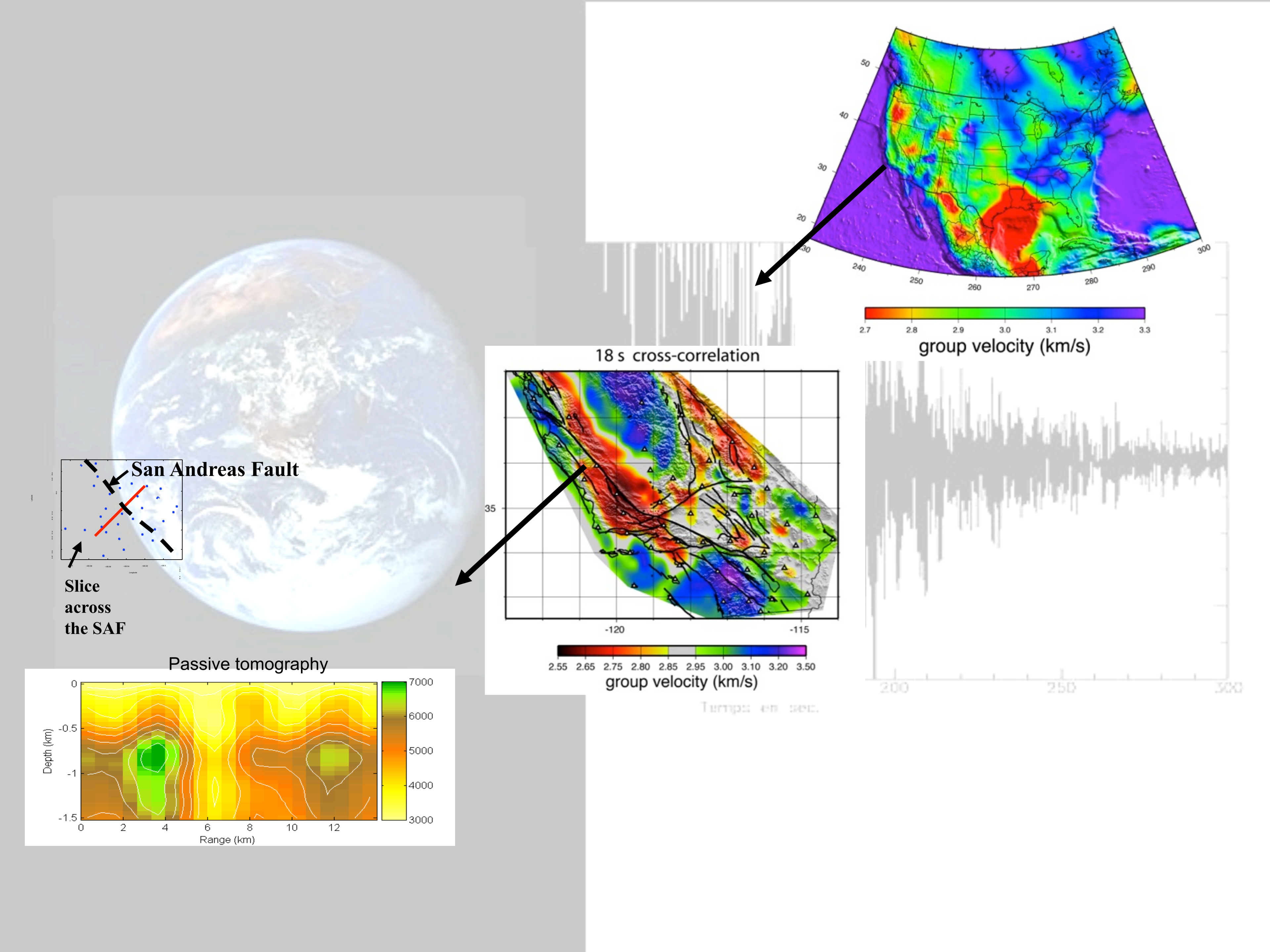

San Andreas Fault
Slice across the SAF
Passive tomography
Depth (km)
Range (km)
0 -0.5 -1 -1.5
0 2 4 6 8 10 12
7000 6000 5000 4000 3000
18 s cross-correlation
35
-120 -115
2.55 2.65 2.75 2.80 2.85 2.95 3.00 3.10 3.20 3.50
group velocity (km/s)
50 40 30 20
240 250 260 270 280 290 300
2.7 2.8 2.9 3.0 3.1 3.2 3.3
group velocity (km/s)

The 'correlation relation' (under the hypothesis of random sources or multiple scattering):

$$\partial_\tau C_{AB}(\tau) \propto G^+(A,B,\tau) - G^-(A,B,-\tau)$$

Average correlation of fields in A and B

Green function between A and B (for positive and negative times)

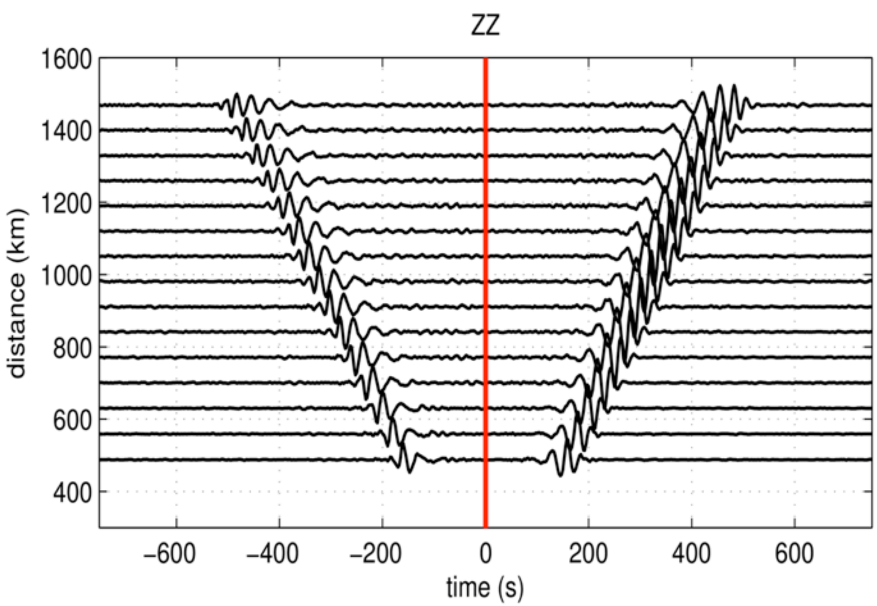

Superposition of G(t) and G(-t)…….

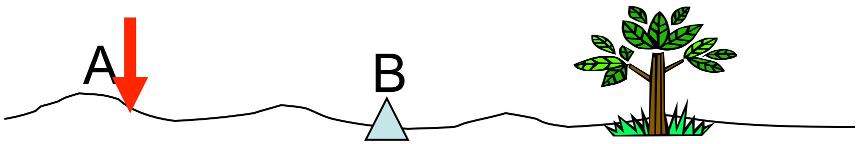

Rayleigh waves across USArray
(from P. Boué, UJF)

Surface wave imaging with ambient seismic noise….. it works!

Map of Rayleigh wave group velocity in California

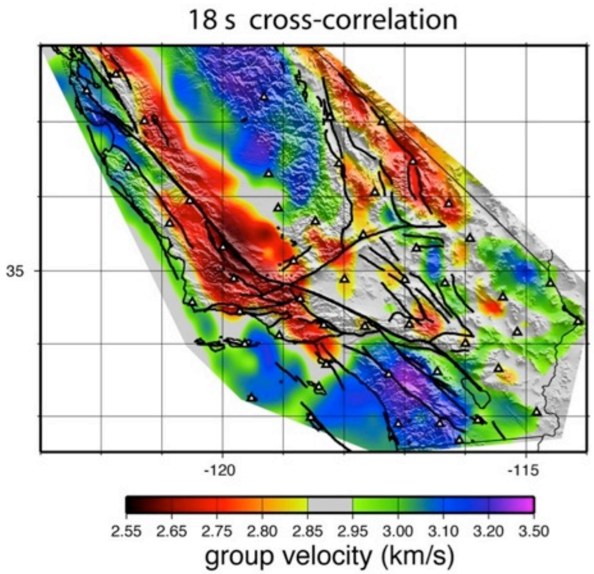

Shapiro et al. , 2005.

The Moho beneath the Alps

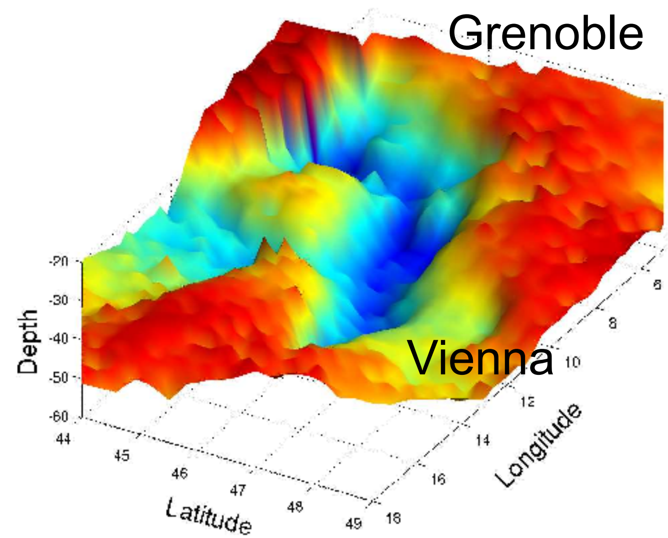

Stehly et al. ,2009

Indeed, the quality depends on the distribution of 'noise' sources:

-analysis of specific noise characteristics

-the technique is robust for smooth azimuthal distributions of noise intensity

-clock errors detection and correction by time symmetry

-use of information redundancy:

9 component correlation tensor

positive and negative time vs. time symmetry

Surface wave imaging with ambient seismic noise….. it works!

Map of Rayleigh wave group velocity in California

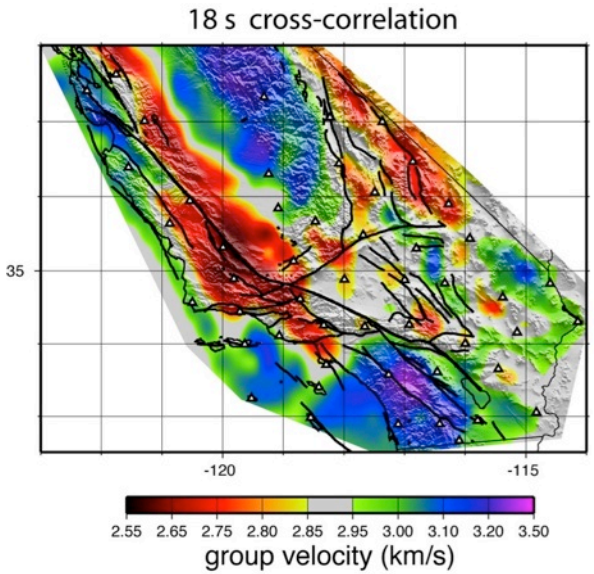

Shapiro et al. Science 2005.

The Moho beneath the Alps

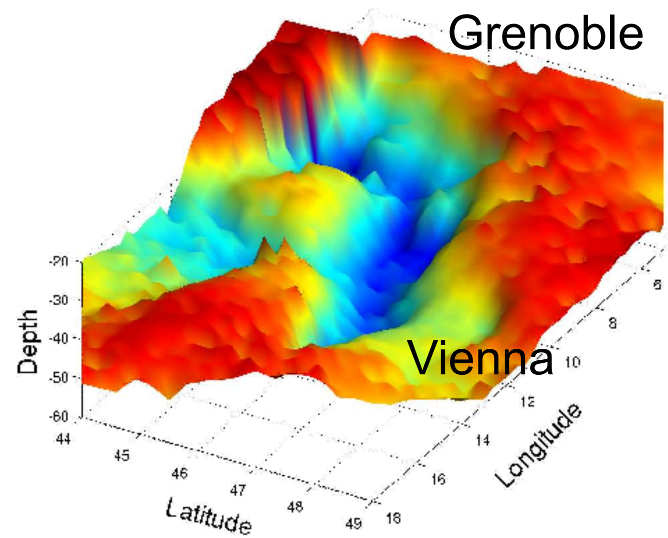

Stehly et al. GJI 2009

Ambient noise imaging complements the traditional approaches.
It is particularly useful for the surface wave tomography of the crust and upper mantle.

Can we use the noise for body wave imaging as well?

The smaller is the contribution of a specific arrival to the Earth response, the more difficult is its reconstruction.

It was worth trying….

The search for body waves : crustal propagation (e.g. Draganov et al., 2009; Zhang et al., 2010, Poli et al.,

➔Earth's mantle discontinuities from ambient seismic noise

Poli et al. Science 2012

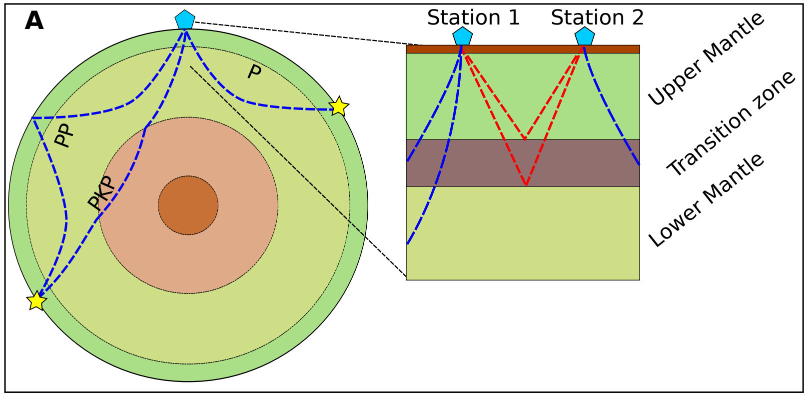

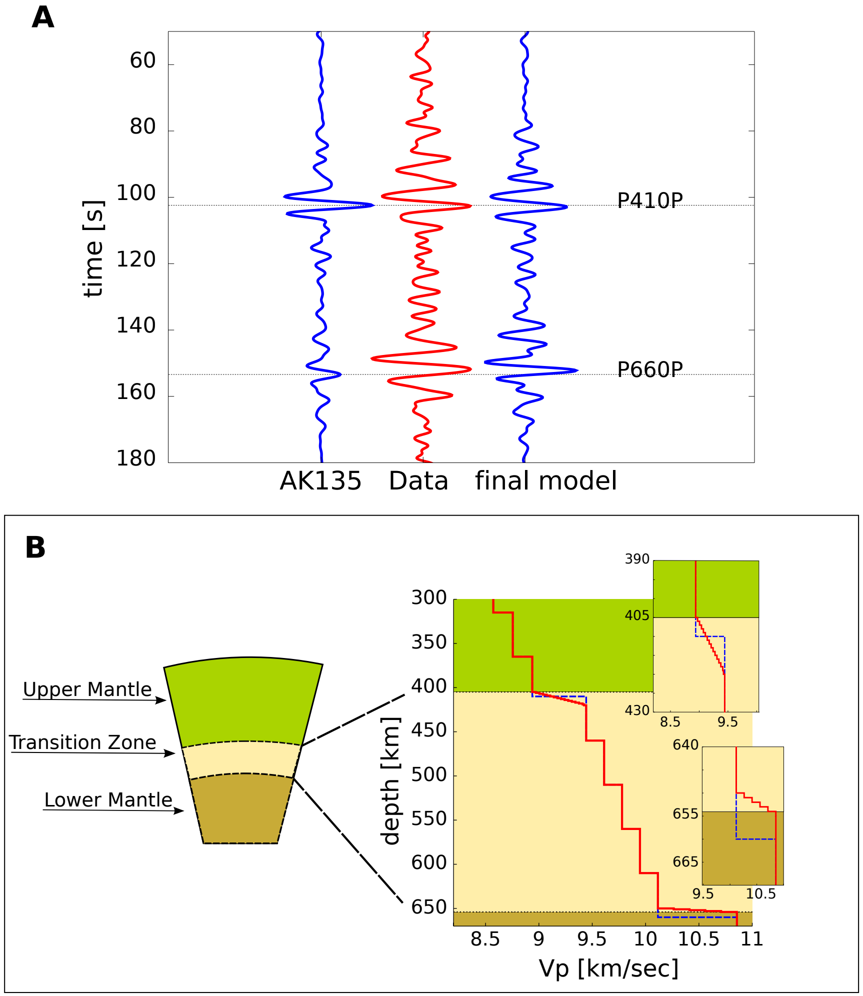

Monitoring the elastic properties of the rocks

Correlation functions as approximate Green functions
(ex: period band:2-8s Parkfield, Brenguier et al., 2008)

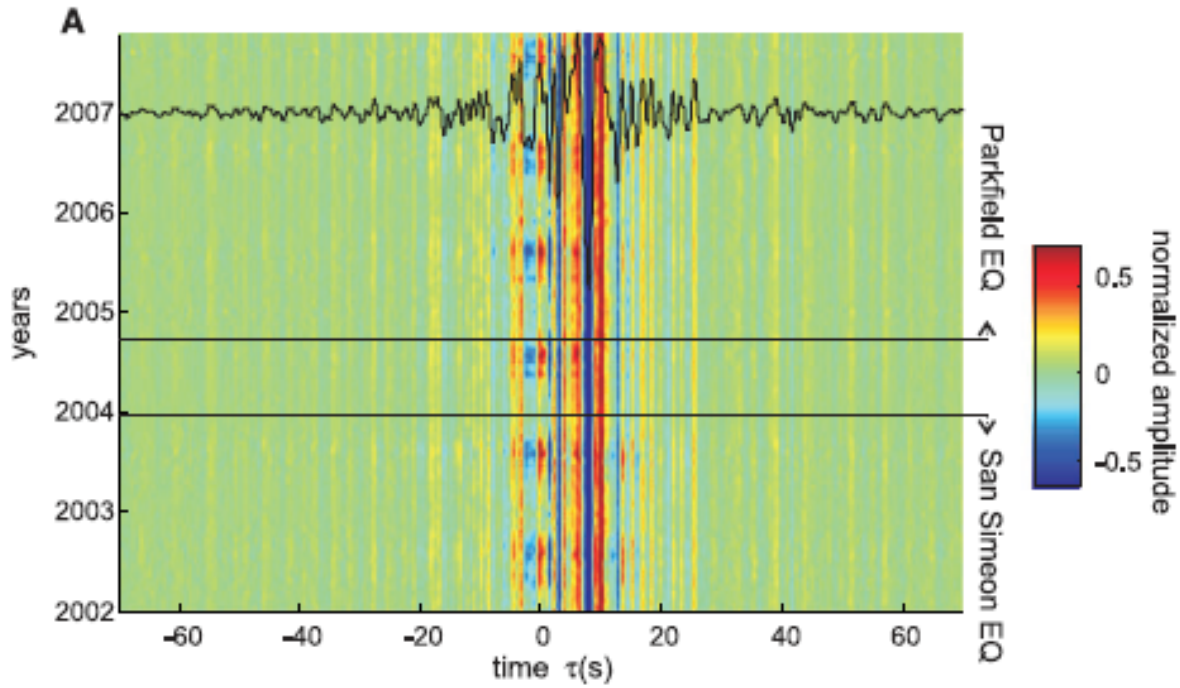

Direct waves are sensitive to noise source distribution (relative errors small enough for tomography (≤1%) but too large for monitoring (goal ≈ 10^{-4})

Stability of the ‘coda’ of the noise correlations = frozen distribution of scatterers

We can construct virtual seismograms between stations pairs from noise records.

They contain the information about structures, but also all the complexity of actual seismograms (e.g. Weaver and Lobkis 2004)

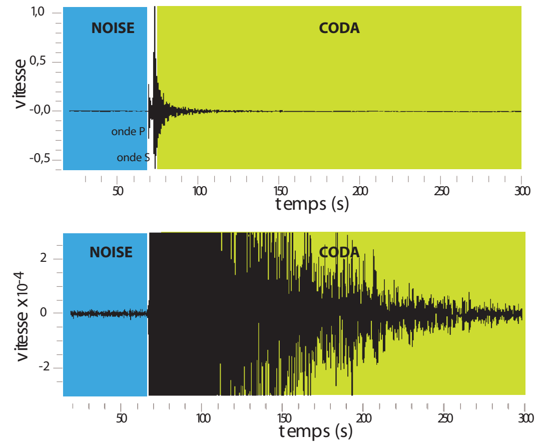

Specifically they contain the scattered waves (coda waves). This is attested by the fact that we can also construct 'virtual' seismograms from the correlation of noise based virtual seismograms

➔ C^3 method *(Stehly et al., 2008; Garnier et al., 2011)*

➔ can even be iterated in C^5.. *(Froment et al., 2011)*

➔ long travel times = strong sensitivity to changes

Detecting a change of seismic speed: coda waves

Comparing a trace with a reference under the assumption of an homogeneous change

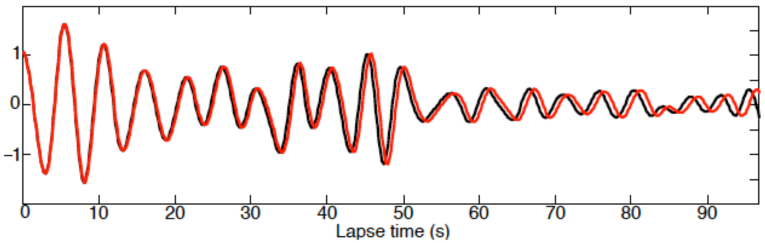

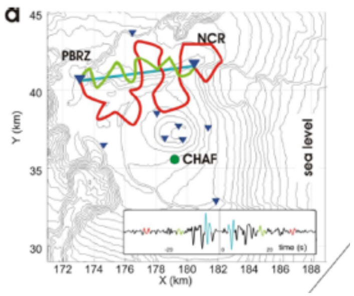

The ‘doublet’ method: moving window cross spectral analysis *(Poupinet et al., 1984; Snieder 2002,*

Variation induced by the Parkfield earthquake

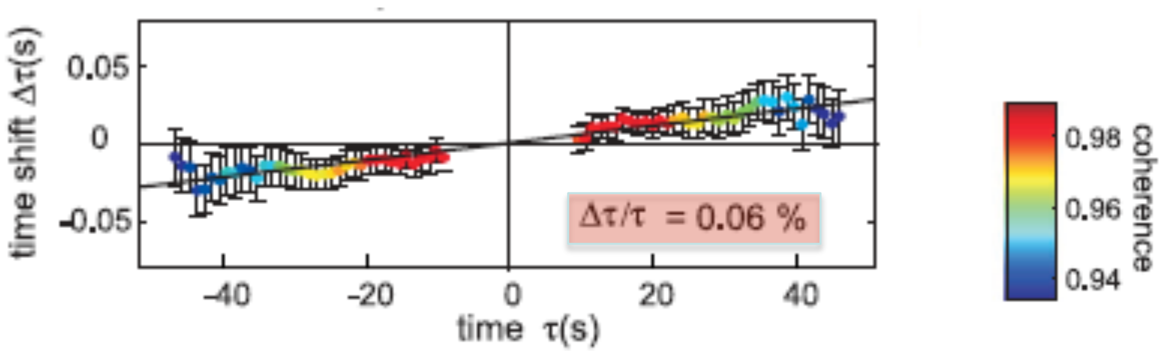

$$\Delta\tau / \tau = -\Delta V / V$$

Alternatively, the stretching method is a global optimization technique

Application Piton de la Fournaise

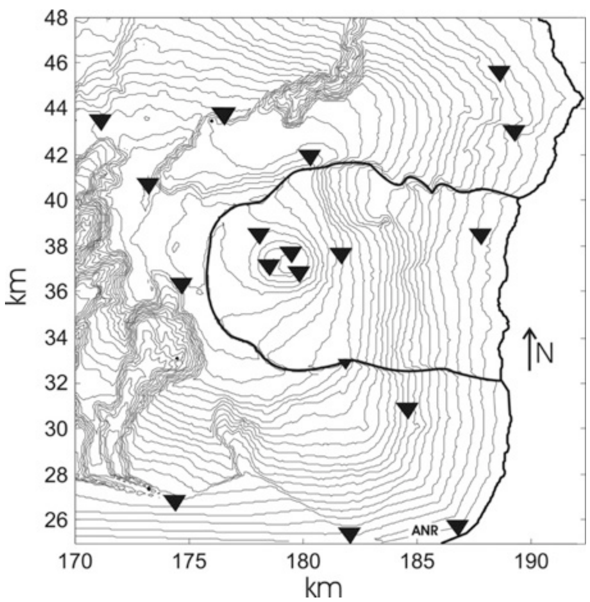

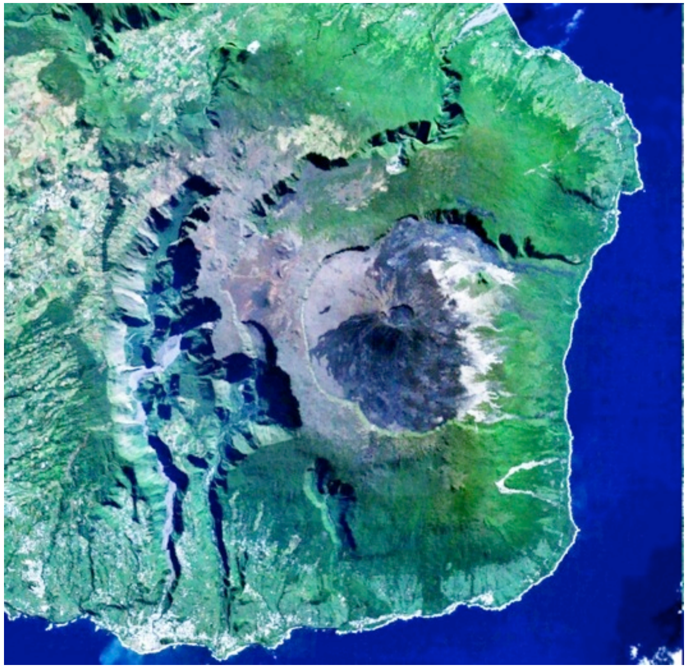

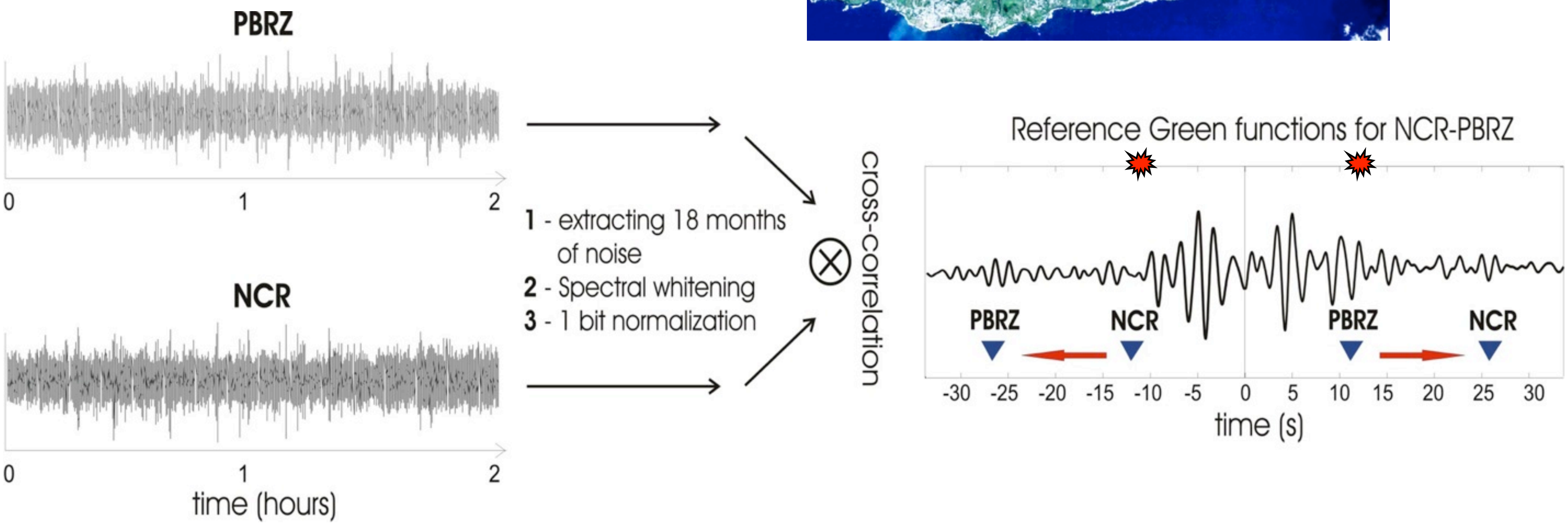

A precursory velocity drop...

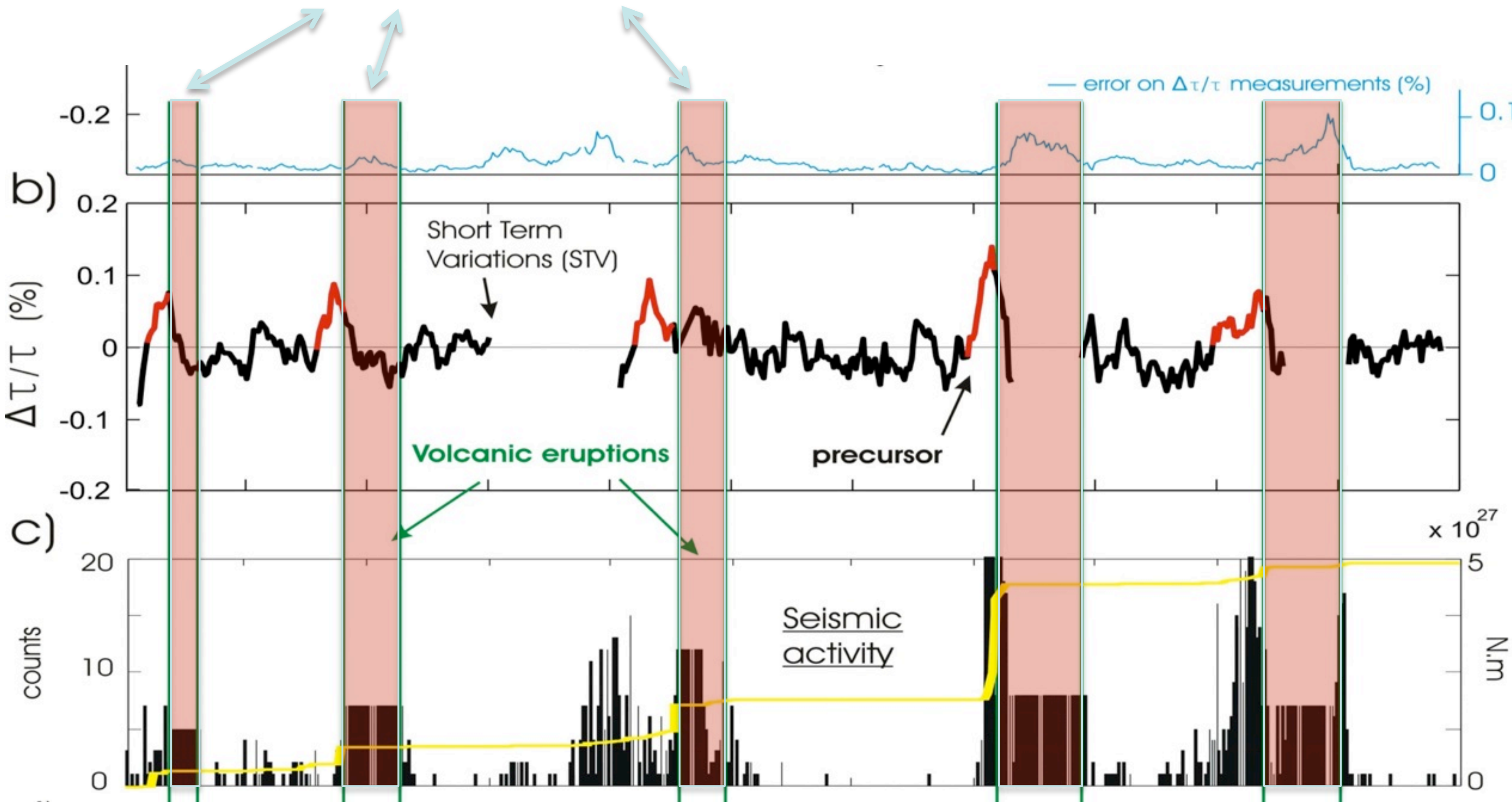

Application to Parkfield *(Brenguier et al. 2008)*
Short period sensors / Processing in the period 1-10s

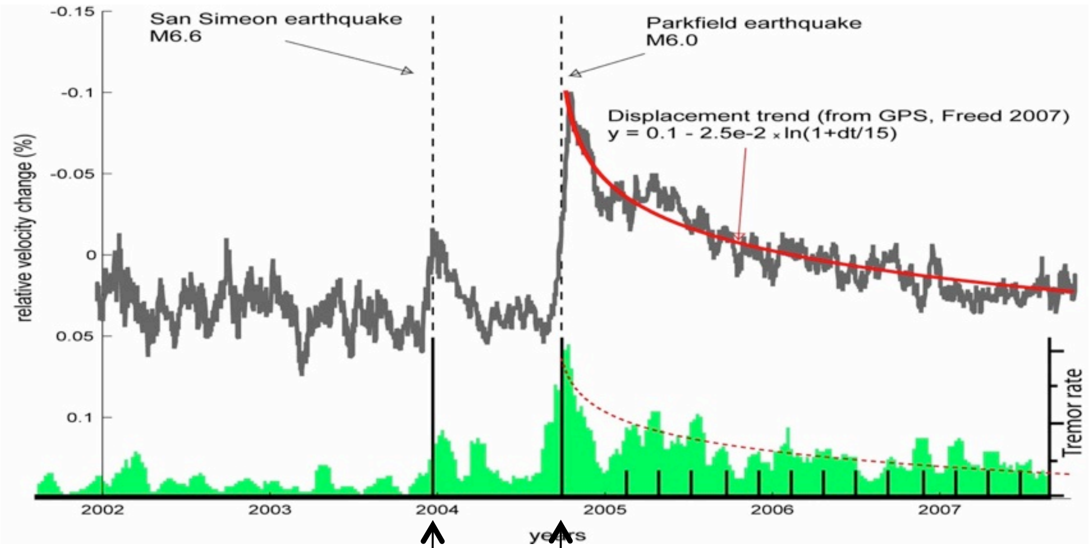

Distant event **Local event**

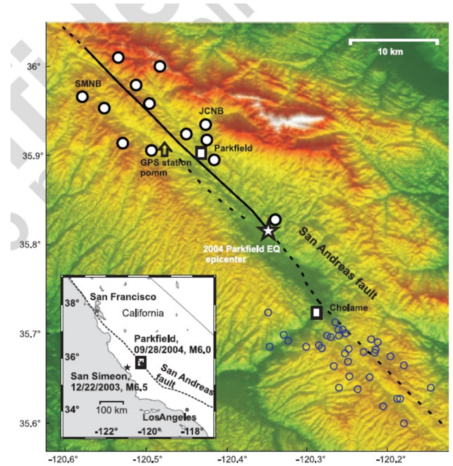

HRSN network

➔ GPS trend
➔ tremor activity